

Quantum correlations across the horizon in acoustic and gravitational black holes

Roberto Balbinot^{*}

*Dipartimento di Fisica dell'Università di Bologna and INFN sezione di Bologna,
Via Imerio 46, 40126 Bologna, Italy*

Alessandro Fabbri[†]

*Departamento de Física Teórica and IFIC, Universidad de Valencia-CSIC,
C. Dr. Moliner 50, 46100 Burjassot, Spain*

 (Received 13 July 2021; accepted 14 January 2022; published 15 February 2022)

We investigate, within the framework of quantum field theory in curved space, the correlations across the horizon of a black hole in order to highlight the particle-partner pair creation mechanism at the origin of Hawking radiation. The analysis concerns both acoustic black holes, formed by Bose-Einstein condensates, and gravitational black holes. More precisely, we have considered a typical acoustic black hole metric with two asymptotic homogeneous regions and the Schwarzschild metric as describing a gravitational black hole. By considering equal-time correlation functions, we find a striking disagreement between the two cases: the expected characteristic peak centered along the trajectories of the Hawking particles and their partners seems to appear only for the acoustic black hole and not for the gravitational Schwarzschild one. The reason for that is the existence of a quantum atmosphere displaced from the horizon as the locus of origin of Hawking radiation together, and this is the crucial aspect, with the presence of a central singularity in the gravitational case swallowing everything is trapped inside the horizon. Correlations, however, are not absent in the gravitational case; to see them, one simply has to consider correlation functions at unequal times, which indeed display the expected peak.

DOI: [10.1103/PhysRevD.105.045010](https://doi.org/10.1103/PhysRevD.105.045010)

I. INTRODUCTION

One of the most amazing properties of black holes (BHs) is that, despite their name, they are not really black as they emit thermal radiation. This is the spectacular result reached by Hawking in 1974 [1], a milestone of modern theoretical physics. Unfortunately, this radiation is so weak that it is almost impossible (at least so far) to reveal it. More precisely, the emission temperature for a solar mass BH is of order 10^{-7} K (which should be compared to the 2.7 K of the cosmic microwave background) and even lower for more massive BHs since this temperature scales inversely proportional to the mass. The only hope could come from primordial BHs [2] whose mass can be significantly lower than the solar mass, but so far, no evidence of such a kind of signals has been revealed (see, for example, Ref. [3]).

The mechanism responsible for the Hawking radiation is intrinsically quantum mechanical, namely, the conversion of quantum vacuum fluctuations in on-shell real particles. More precisely, pairs of correlated particles are created, one member outside the BH horizon escaping to infinity and

constituting the thermal radiation and the other, called partner [4], inside the horizon getting swallowed by the interior singularity. Note that particle and partner have opposite Killing energy, and this allows the mechanism of pair creation to work even in static or stationary space-times.

In 1981, Unruh [5] showed that the same quantum mechanism could work in a fluid crossing the speed of sound, opening the possibility of observing the analog of Hawking radiation in systems less exotic than BHs and manageable in a laboratory. This started the interest in the so-called analog models, condensed matter systems which mimic characteristic features of BHs and the early Universe and which can be used as a laboratory to test the predictions of quantum field theory (QFT) in curved space-times [6]. Most of the research has been concentrated to sonic analog of BHs constructed from Bose-Einstein condensates (BECs) [7] where the expected Hawking temperature ~ 10 nK is only 1 order of magnitude less than the background (~ 100 nK). Nevertheless, competing effects like thermal emission can still cover the Hawking radiation. To overcome this, it was realized that Hawking radiation has a characteristic imprint on the equal-time density-density correlation function when one point is taken outside the

^{*}balbinot@bo.infn.it
[†]afabbri@ific.uv.es

sonic horizon and the other is taken inside [8,9]. Once the horizon is formed and a stationary regime is reached, a well-defined peak appears, reflecting the correlation between the Hawking particles and their partners. This is the smoking gun of the presence of Hawking radiation. Using this input, Steinhauer [10] and de Nova *et al.* [11], by a series of experiments, were finally able to reveal it.

In recent time, the attention of the experimentalists has been moved from the stationary regime, which is theoretically almost understood, to the dynamic formation of time-dependent analog BH horizons, like the experiment reported by Kolobov *et al.* [12]. They were able to follow the ramp-up of Hawking radiation following the formation of a sonic horizon in a BEC looking at the time evolution of the in-out density correlation function. In this paper, we will show how, using the powerful methods of QFT in curved space-times, one can theoretically describe this ramp-up. This is done in a simple toy model of the sonic BH formation, which allows an analytical treatment able to reproduce the qualitative features of the experiment [13]. The temporal evolution of the in-out correlation function toward its stationary configuration we obtain will shed light on when and where Hawking radiation emerges out of the vacuum fluctuations.

Locating the origin of Hawking radiation in a BH is a long-standing issue. It was first discussed by Unruh [14], analyzing the propagation of the modes associated to a quantum field in a BH space-time. Later, Giddings [15] introduced the idea of a quantum atmosphere significantly displaced from the horizon as the locus where Hawking radiation emerges out of vacuum fluctuations. This work was followed by other authors refining the analysis [16,17]. The results of these studies locate in a Schwarzschild black hole the region where the Hawking particles emerge at a distance $O(1/\kappa)$ from the horizon, where κ is the horizon's surface gravity. We will see that our analysis based on correlation across the horizon will give strong support on the existence of a quantum atmosphere also for acoustic BHs.

Usually, the studies on Hawking radiation for gravitational BHs focus on the region exterior to the horizon. One looks, for example, to the particle spectrum revealed far away from the BH, analyzing the modes of the quantum field associated to the emitted particles and the related Bogoliubov transformations [1]. At a deeper level, one tries to get information on Hawking radiation by studying the renormalized stress-energy tensor of the quantum field [18].

Here, inspired by the work on acoustic BHs, we will also study the particle-partner correlation across the horizon in Hawking radiation for a BH formed by gravitational collapse. Of course, one has no access to the region inside the horizon since this surface is now a causal boundary preventing the information from the inside from leaking outside. So, this study has just a theoretical interest.

Nevertheless, the complete different pattern of the equal-time in-out correlations, which will emerge compared to the ones in acoustic BHs because of the presence of an interior singularity, will help us to understand better the role of the quantum atmosphere in the Hawking effect.

The paper is organized as follows. In Sec. II, we discuss the correlations across the horizon of the density fluctuations in an acoustic BH formed by a BEC. The toy model used to mimic the horizon formation and the technical details are left in Appendix A. In Sec. III, the same kind of analysis is performed for a BH formed by gravitational collapse of a null shell. Some mathematical details are given in Appendix B. Section IV is devoted to the conclusions.

II. IN-OUT CORRELATIONS IN BEC SONIC BLACK HOLES

In Ref. [13], we have shown, using a simple model, how, with the methods of QFT in curved space, one can describe quite well the time evolution of the density-density correlation function in a BEC once a sonic horizon is formed (see also Refs. [19,20]). The goal was to locate where and when the signal of the presence of Hawking radiation appears.

In this paragraph, we review the model and discuss the results. The technical details are given in Appendix A.

The model we use to mimic the BH formation is quite simple so that a complete analytical treatment is possible. However, we are confident that its outcomes describe, at least qualitatively, correctly the physics of the ramp-up of Hawking radiation toward the stationary regime characterized by the peak in the correlation function mentioned in the Introduction.

We assume a one-dimensional BEC flow, directed from right to left along the x axis at a constant velocity $V(<0)$; the density n of the condensate is also constant. By properly modulating the speed of sound c , we can generate the formation of an acoustic BH. To this end, the profile of c is assumed to vary in time as

$$\begin{cases} c = c_{\text{in}}, & t < 0 \\ c = |V| \left(1 + \gamma \tanh \frac{\kappa x}{\gamma |V|} \right), & t > 0, \end{cases} \quad (2.1)$$

where $c_{\text{in}}(>|V|)$ is constant like κ and $\gamma = \frac{2}{3}$. The chosen profile describes a uniform subsonic flow for $t < 0$. At $t = 0$, a sonic BH forms; the region $x > 0$ remains subsonic, while for $x < 0$, the flow is supersonic. The sonic horizon is located at $x = 0$, and κ is its surface gravity. We remark that modulations of the speed of sound in a BEC, even suddenly, are now obtained with routine procedures in laboratories: for example, using Feshbach resonances to vary the atom-atom interaction coupling [21].

The equal-time correlator $G_2^{(1)}(t; x, x')$ of the one-dimensional (1D) density fluctuation operator can be approximated within the gravitational analogy using the methods of QFT in curved space as [8]

$$G_2^{(1)}(t; x, x') = \sqrt{\frac{n(x)n(x')}{m^2 c^3(x)c^3(x')}} \lim_{t \rightarrow t'} D \langle \delta \hat{\theta}^{(2)} \delta \hat{\theta}^{(2)} \rangle, \quad (2.2)$$

where $n(x)$ is the 1D density of the condensate (constant in our model), m is the mass of the single atom of the BEC, D is the differential operator

$$D = (\partial_t + V\partial_x)(\partial_{t'} + V\partial_{x'}), \quad (2.3)$$

and $\langle \delta \hat{\theta}^{(2)}(t, x) \delta \hat{\theta}^{(2)}(t', x') \rangle$ is the two-point function of a 1 + 1-dimensional massless scalar field $\delta \hat{\theta}^{(2)}$, whose field equation is

$$\hat{\square} \delta \hat{\theta}^{(2)} = 0, \quad (2.4)$$

propagating in the 1 + 1D acoustic metric

$$ds^2 = -(c^2 - V^2)dt^2 - 2Vtdt dx + dx^2, \quad (2.5)$$

and $\hat{\square}$ is the covariant d'Alembert operator computed from the above metric.

This approximation neglects backscattering of the modes caused by the inhomogeneity of the BEC (i.e., curvature of

the acoustic metric) [22]. This backscattering produces two secondary peaks in the correlation pattern besides the main one referred to in the Introduction [23–25], but so far, no experiment has been able to see them, given the much weaker signature of these ones compared to the former. The mathematical details of our construction are given in Appendix A. Here, we discuss the results we have obtained. In Fig. 1, we plot $G_2^{(1)}(t; x, x')$ for points $x > 0$ (outside the horizon) and $x' < 0$ (inside the horizon) at four increasing times, $t_1 = 1/\kappa$, $t_2 = 2/\kappa$, $t_3 = 4/\kappa$, and $t_4 = 5/\kappa$.

At late time, once the stationary regime is achieved, a peak at $x' = -x$ is expected, signaling the correlation of the Hawking particles and their partners. The signal is the one that has been experimentally observed [10–12]. In our model, the late-time limit is governed by the condition $e^{-\kappa t} \sinh \frac{3\kappa|x|}{2|V|} = cst \ll 1$ [see Eq. (A22)]. Note that this condition is reached earlier in the near-horizon region and then it spreads out. From Fig. 1, where we plot the absolute value of $G_2^{(1)}(t; x, x')$ (the correlator is negative), one sees indeed the formation of a peak located at $x' = -x$. Note, however, that this holds for $x = -x'$ sufficiently far away from the horizon. To see this more clearly, in Fig. 2, we plot the correlator evaluated at $t = \frac{10}{\kappa}$ as a function of x for various fixed points x' : $x' = -5, -6, -7, -8$. The peak is located at $x = -x'$ only for $|x'| \gtrsim 7|V|/4\kappa$. For values of x' closer to the horizon, the peak does not appear. So, there is no sign of correlations in the near-horizon region.

Let us understand the reason. The correlator is given [see Eq. (A19)] by

$$\begin{aligned} G_2^{(1)}(t; x, x') &= -\frac{\hbar n}{4\pi m c(x)^{1/2} c(x')^{1/2}} \left[\frac{1}{(c(x) - |V|)(c(x') - |V|)} \frac{du_{\text{in}} du'_{\text{in}}}{du du'} \frac{1}{(u_{\text{in}} - u'_{\text{in}})^2} \right. \\ &\quad \left. + \frac{1}{(c(x) + |V|)(c(x') + |V|)} \frac{dv_{\text{in}} dv'_{\text{in}}}{dv dv'} \frac{1}{(v_{\text{in}} - v'_{\text{in}})^2} \right] \Big|_{t=t'} \\ &\equiv G_{2,u}^{(1)}(t; x, x') + G_{2,v}^{(1)}(t; x, x'). \end{aligned} \quad (2.6)$$

The relevant term is the first one in Eq. (2.6) describing the correlations of the positive (Killing) energy Hawking particles and their negative (Killing) energy partners. Let us call this term $G_{2,u}^{(1)}(t; x, x')$. The other one $G_{2,v}^{(1)}(t; x, x')$ is related to the v sector.

At late advanced time, we have $u_{\text{in}} = \pm \frac{e^{-\kappa u}}{|A|}$ [see Eq. (A12)], where the minus sign refers to points outside the horizon ($x > 0$) and the plus sign refers to points inside the horizon ($x < 0$). In this limit, we have

$$G_{2,u}^{(1)}(t; x, x') = -\frac{\hbar n \kappa^2}{4\pi m V^2 \gamma^2 \sqrt{c(x)c(x')}} \frac{\cosh \beta x \cosh \beta x'}{(\sinh \beta x - \sinh \beta x')^2}, \quad (2.7)$$

where $\beta \equiv \frac{\kappa}{\gamma|V|}$. For x and x' far away from the horizon, the absolute value of $G_{2,u}^{(1)}(t; x, x')$ has a local maximum at $x = -x'$, while for $x, x' \rightarrow 0$, we have

$$\begin{aligned} \lim_{x, x' \rightarrow 0} G_{2,u}^{(1)}(t; x, x') &= -\frac{\hbar n}{4\pi m |V|} \frac{1}{(x - x')^2} \\ &= \lim_{x, x' \rightarrow 0} G_{2,v}^{(1)}(t; x, x'). \end{aligned} \quad (2.8)$$

Away from the horizon, $G_{2,v}^{(1)}(t; x, x')$ rapidly decreases, see Fig. 3, and becomes one order of magnitude smaller than $G_{2,u}^{(1)}(t; x, x')$.

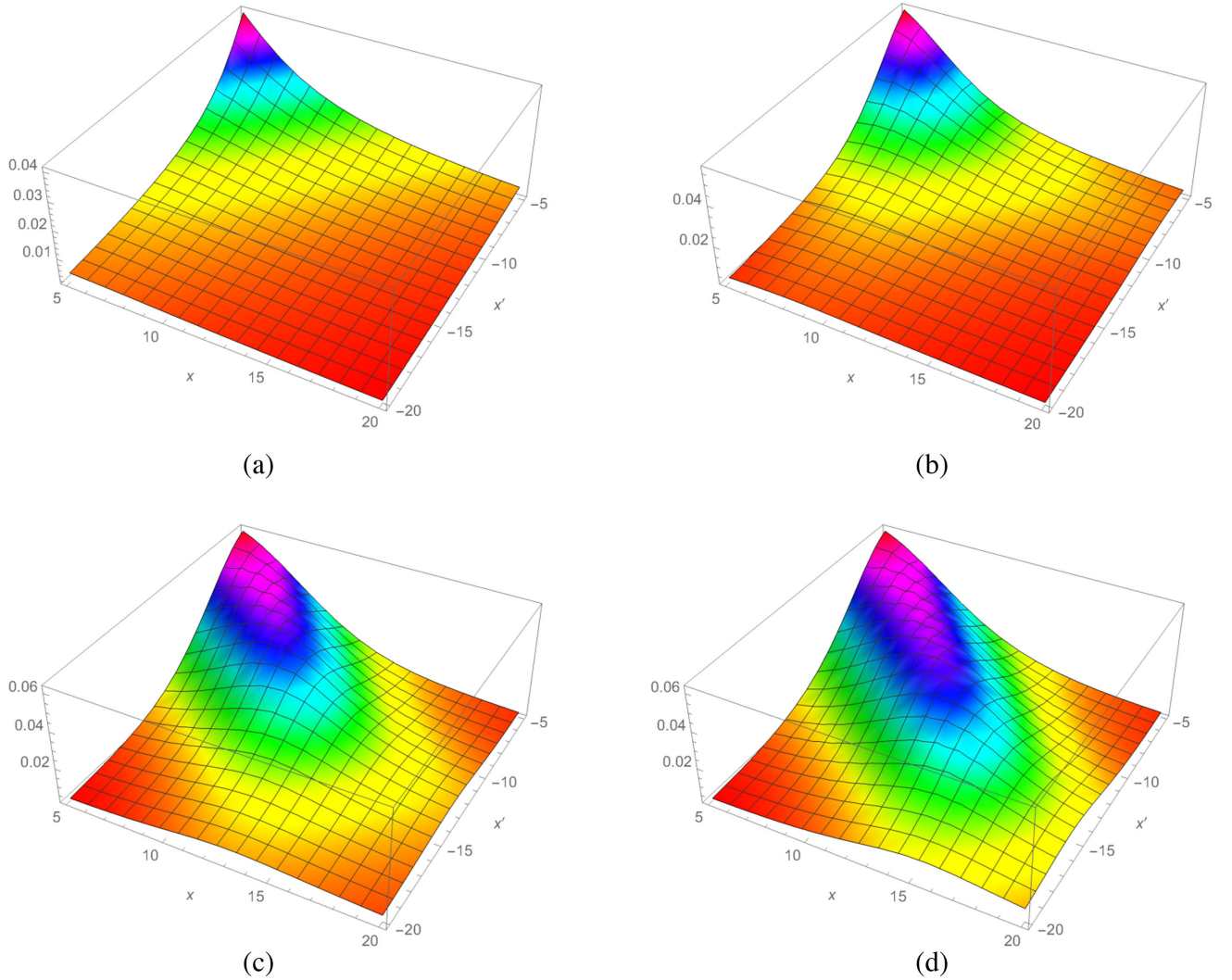


FIG. 1. Plots of the absolute value of $G_2^{(1)}(t; x, x')$, for $x > 0$ (outside the horizon) and $x' < 0$ (inside the horizon), at four increasing times $t_1 = 1/\kappa$ (a), $t_2 = 2/\kappa$ (b), $t_3 = 4/\kappa$ (c), $t_4 = 5/\kappa$ (d). Here and in the figures that follow in this section, we plot the correlator up to the overall factor $\frac{\hbar\eta}{4\pi m}$ and have chosen the values $\kappa = \frac{1}{4}$, $|V| = 1$, $c_{\text{in}} = \frac{3}{2}$.

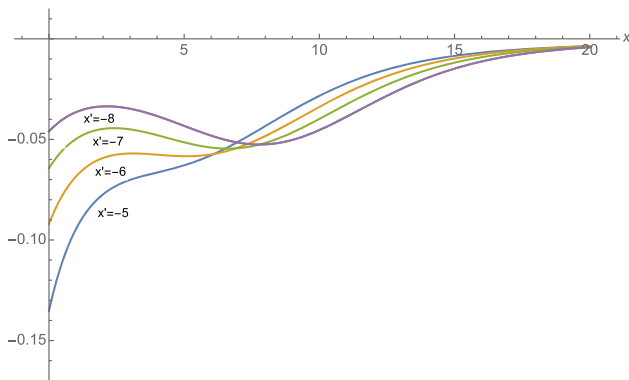


FIG. 2. Plot of $G_2^{(1)}(t; x, x')$ at $t = \frac{10}{\kappa}$, as a function of x for various (indicated) fixed x' .

From these considerations, we can deduce that for x, x' close to the horizon the light-cone singularity of the two-point function starts dominating and the local minimum disappears (see Fig. 2) [26]. The correlator describes just diverging vacuum fluctuations as $x = -x' \rightarrow 0$. So, we see that the emergence of the Hawking's particle-partner pair creation out of vacuum fluctuations does not occur close to the horizon but in a region, named “quantum atmosphere” by Giddings [15], outside the horizon which within our model can be located at $x = -x' \sim 7$ and which corresponds to a distance of $\frac{7|V|}{4\kappa}$. One important aspect that also emerges is that the peak signal does not appear immediately after the formation of the horizon ($t = 0$) but after a characteristic time of the order $4/\kappa$.

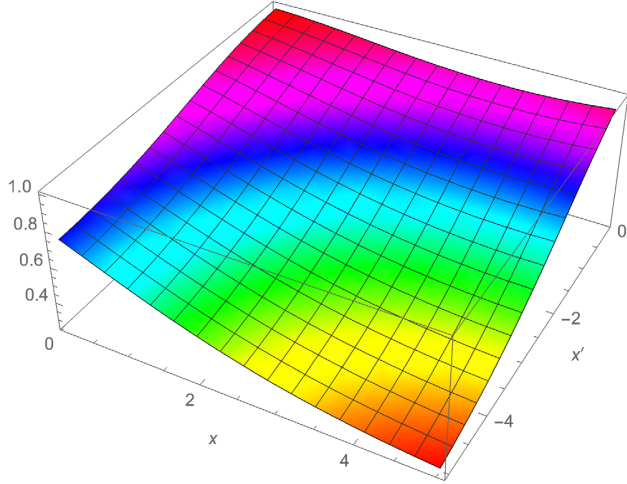


FIG. 3. $\frac{G_{2,e}^{(1)}(t;x,x')}{G_{2,u}^{(1)}(t;x,x')}$, defined by (2.6), at $t = \frac{10}{\kappa}$ in the near-horizon region.

To reveal the correlations close to the horizon, one needs to consider the correlator no longer at equal times. At late time, we have

$$G_{2,u}^{(1)}(t, t'; x, x') = -\frac{\hbar n \kappa^2}{4\pi m V^2 \gamma^2 \sqrt{c(x)c(x')}} \times \frac{\cosh \beta x \cosh \beta x'}{(e^{-d} \sinh \beta x - e^d \sinh \beta x')^2}, \quad (2.9)$$

where $d = \frac{\kappa}{2}(t - t') \equiv \frac{\kappa}{2} \Delta t$.

In Fig. 4, we plot the absolute value of the unequal time correlator (2.9) at three increasing Δt ($= 1/2\kappa, 1/\kappa, 3/2\kappa$) intervals and, in Fig. 5, we plot it as a function x for five different values of x' .

One sees that the values of x' at which the peak appears decreases toward the horizon as Δt increases, while for large enough x , x' , the peak is located at $u = u'$, i.e.,

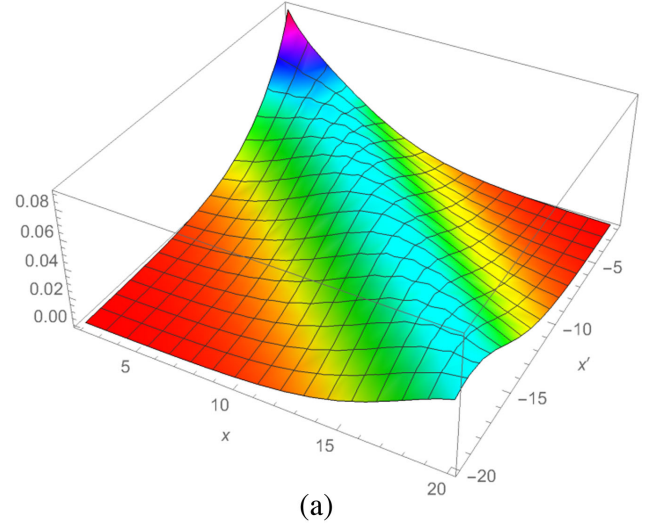
$$u = t - \frac{1}{\kappa} \ln \sinh \beta x = t' - \frac{1}{\kappa} \ln \sinh |\beta x'|, \quad (2.10)$$

along the trajectories of the Hawking particle and its partner as expected.

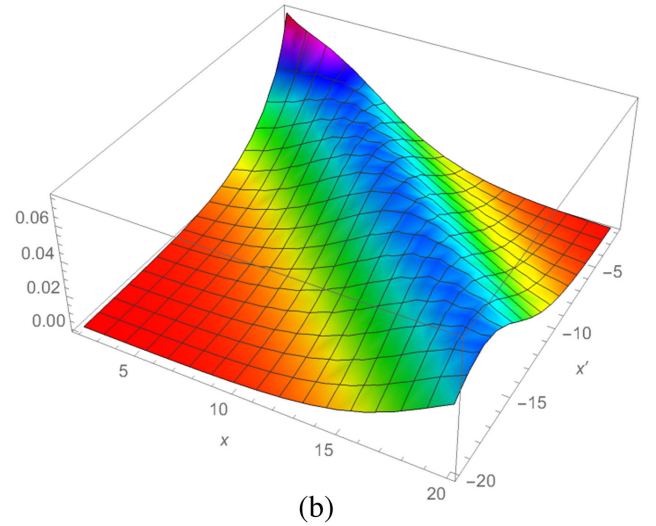
The analysis we have performed so far considered a BEC whose temperature is zero. Experimentally, this is difficult to achieve, so one should consider the case in which the condensate has an initial temperature $T \neq 0$. So, for $t < 0$, we have a thermal distribution of phonons characterized by an occupation number,

$$N_{\omega_{u(v)}} = \frac{1}{e^{\frac{\hbar \omega_{u(v)}}{k_B T}} - 1}, \quad (2.11)$$

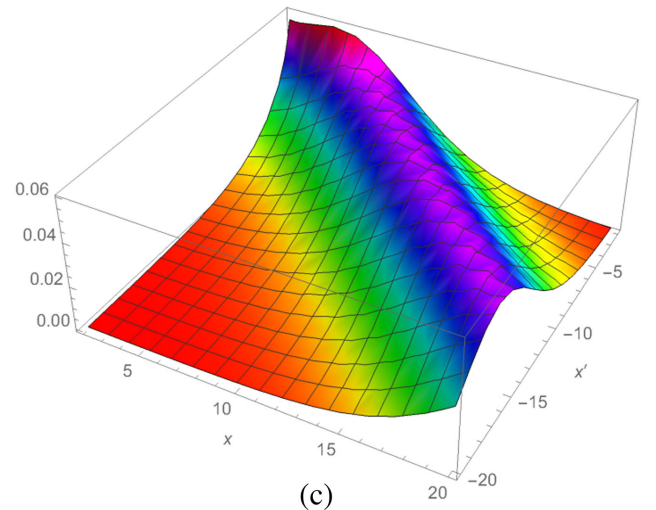
where



(a)



(b)



(c)

FIG. 4. Absolute value of the unequal-time correlator (2.9) at three increasing Δt [$= 1/2\kappa$ (a), $1/\kappa$ (b), $3/2\kappa$ (c)] intervals.

$$\omega_u = \frac{\omega c_{\text{in}}}{c_{\text{in}} - |V|}, \quad \omega_v = \frac{\omega c_{\text{in}}}{c_{\text{in}} + |V|} \quad (2.12)$$

are the Doppler rescaled frequencies. The corresponding equal-time correlator is given now (see Appendix A) as

$$G_{2T}^{(1)}(t; x, x') = -\frac{\hbar n}{4\pi m c(x)^{1/2} c(x')^{1/2}} \left[\frac{1}{(c(x) - |V|)(c(x') - |V|)} \frac{du_{\text{in}} du'_{\text{in}}}{du du'} \frac{A_u^2}{\sinh^2 A_u(u_{\text{in}} - u'_{\text{in}})} \right. \\ \left. + \frac{1}{(c(x) + |V|)(c(x') + |V|)} \frac{dv_{\text{in}} dv'_{\text{in}}}{dv dv'} \frac{A_v^2}{\sinh^2 A_v(v_{\text{in}} - v'_{\text{in}})} \right] \Big|_{t=t'}, \quad (2.13)$$

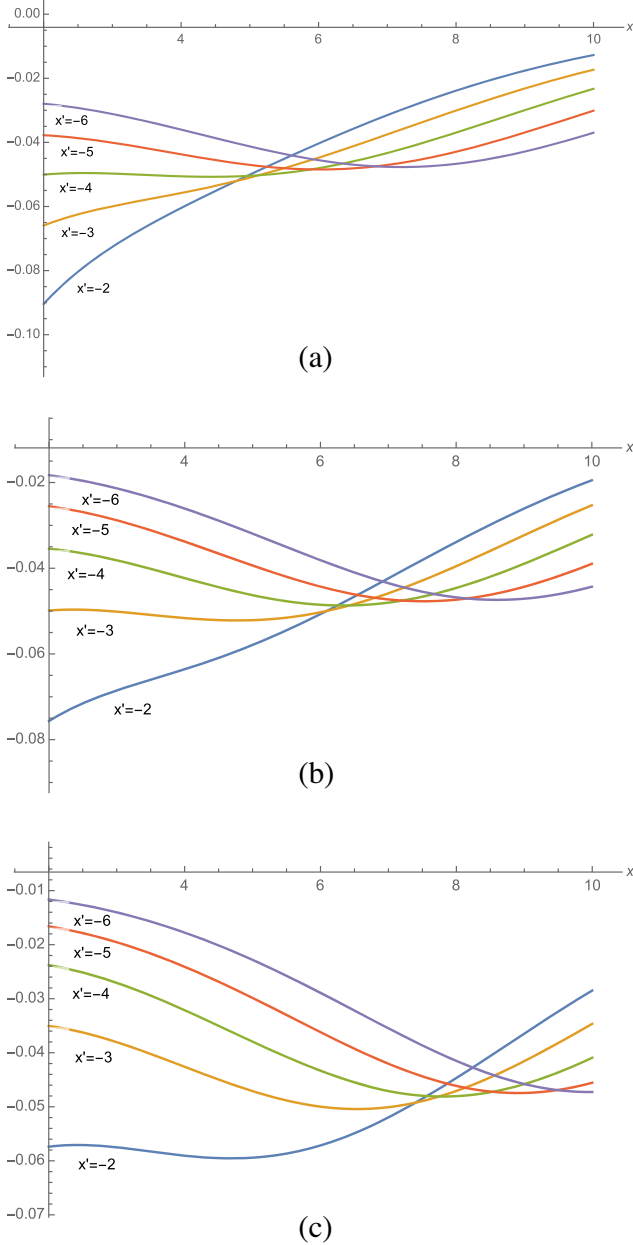


FIG. 5. Unequal-time correlator (2.9) as a function of x for five different fixed values of x' at three increasing Δt [$= 1/2\kappa$ (a), $1/\kappa$ (b), $3/2\kappa$ (c)] intervals.

where

$$A_{u(v)} = \frac{\pi k_B T (c_{\text{in}} \mp |V|)}{\hbar c_{\text{in}}}. \quad (2.14)$$

In Fig. 6, we have the three-dimensional plots of $G_{2T}^{(1)}(t; x, x')$ for $T = T_H$, and in Fig. 7, we have them for $T = 10T_H$ for the same times of Fig. 1.

We see that the ramp-up process to the stationary peaks configuration is slower. The delay grows as the temperature increases. For $T = 10T_H$, the signal appears at $t \sim 5/\kappa$. In Fig. 8, we show $G_{2T}^{(1)}(t; x, x')$, $T = T_H$ in Fig. 8(a) and $T = 10T_H$ in Fig. 8(b), at $t = \frac{10}{\kappa}$ as a function of x for various values of x' as we did in Fig. 2 for the $T = 0$ case.

As shown in Appendix A [see Eq. (A35)], at late time, the first term in Eq. (2.13), $G_{2T,u}^{(1)}(t; x, x')$, which is the dominant one giving the contribution of the u sector, reduces to the corresponding one at $T = 0$ in the same limit. This is a manifestation of the quantum version of the no-hair theorem for BHs (see, for example, Ref. [27]). Hawking radiation at late times is unaffected by any population in the initial state, which causes just a transient stimulated emission [28]. This is because the modes responsible for the late-time behavior in the u channel are the ones with $u \rightarrow \infty$; i.e., they propagate very close to the horizon and are highly redshifted in their journey toward the asymptotic region washing out any information on the initial state. The temperature dependence at late times comes only from the v channel, i.e., $G_{2T,v}^{(1)}(t; x, x')$, but its contribution to the total $G_{2T}^{(1)}(t; x, x')$ is negligible [for $T = T_H$, it is 1 order of magnitude smaller than $G_{2T,u}^{(1)}(t; x, x')$ and decreases by increasing T]. Finite temperature corrections are therefore small within the gravitational approximation.

III. GRAVITATIONAL BLACK HOLES

In this section, in analogy with what we did for the acoustic BEC BH, we shall investigate correlations between the Hawking particles and their partners across the horizon in a real gravitational BH. The striking difference is that the horizon is now a causal boundary preventing any information on inside events to leak

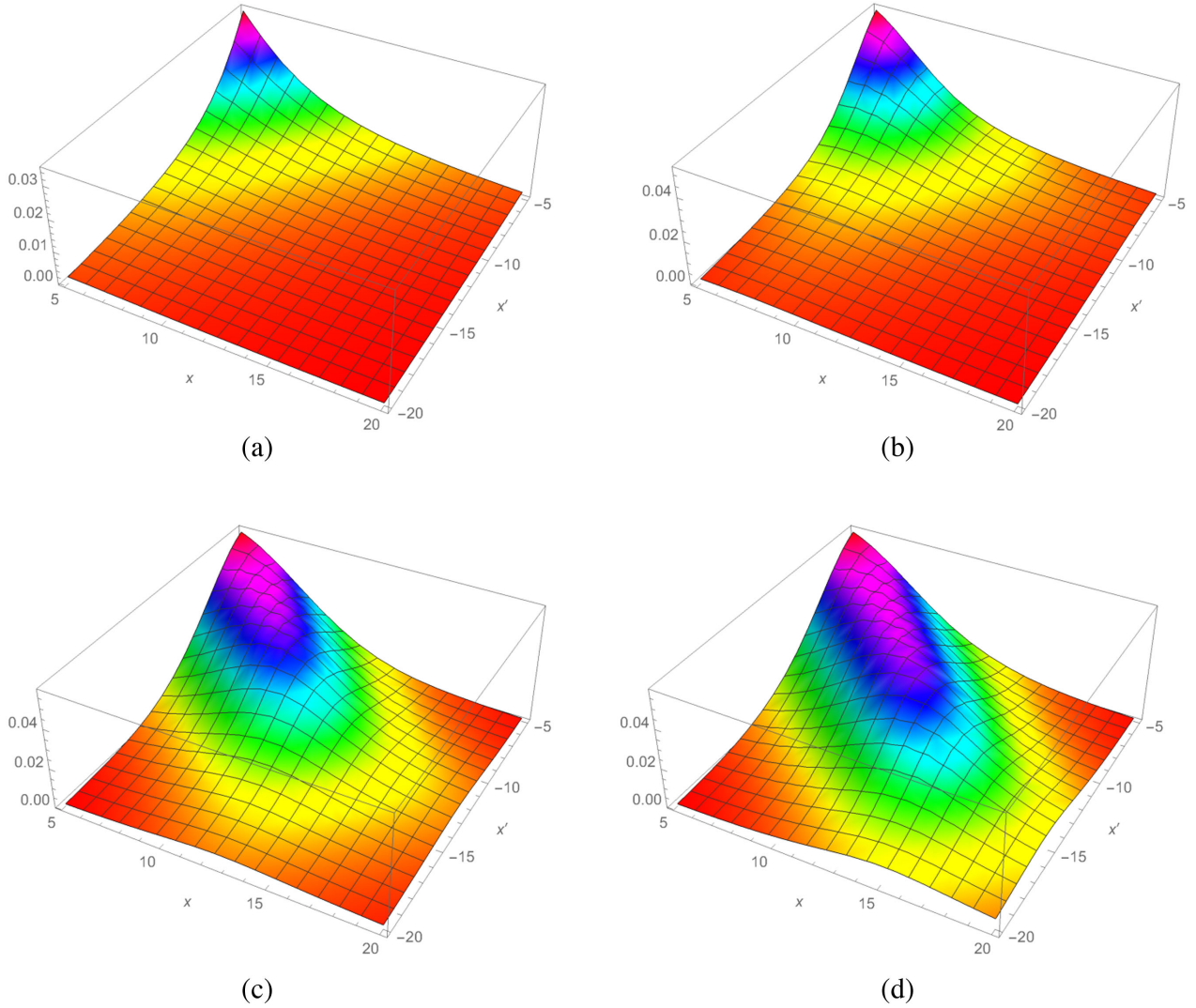


FIG. 6. Three-dimensional plots of the absolute value of $G_{2T}^{(1)}(t; x, x')$ for $T = T_H$ at the same different times of Fig. 1, i.e., $t_1 = 1/\kappa$ (a), $t_2 = 2/\kappa$ (b), $t_3 = 4/\kappa$ (c), $t_4 = 5/\kappa$ (d).

outside. The study of these correlations has therefore only theoretical interest since one cannot perform experiments (even “gedanken” ones) which require measurements whose results can be exchanged by the observers both in the exterior and in the interior of a BH. Nevertheless, as we shall see, the theoretical results of our investigation will turn out to be, at a preliminary inspection, rather unexpected and in strong disagreement with what one finds in the BEC case reviewed in the previous section.

However, one should keep in mind that, although the near-horizon geometry of an acoustic BH is similar to the real one of a gravitational BH, the inner region of an acoustic BH is, in principle (at least in the experiments performed so far), infinite, while the one of a real BH terminates rapidly in a singularity. This fact has a tremendous impact on the correlation functions since these are

genuinely nonlocal quantum objects and as such they do not probe just the local space-time geometry.

We shall begin by considering a very simple toy model of BH formation widely used in the gravitational literature, namely, the collapse of a null shell of radiation (see, for example, Ref. [29]). The shell is located at $v = v_0$, where v is an advanced null coordinate. The space-time metric of this model can be given simply in the Vaidya form

$$ds^2 = -\left(1 - \frac{2M(v)}{r}\right)dv^2 + 2dvdr + r^2(d\theta^2 + \sin^2\theta d\varphi^2), \quad (3.1)$$

where the mass function $M(v)$ has the form

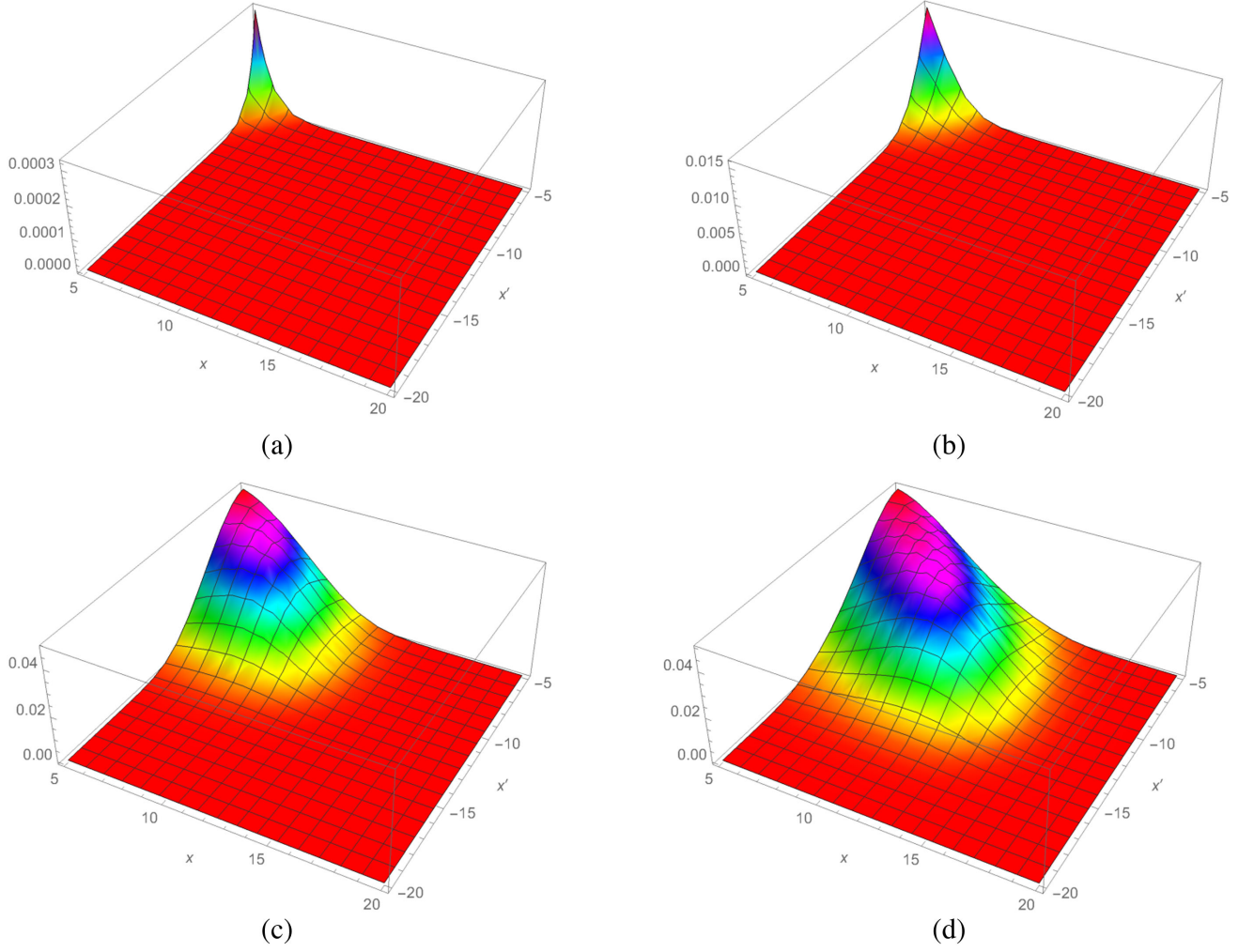


FIG. 7. Three-dimensional plots of the absolute value of $G_{2T}^{(1)}(t; x, x')$ for $T = 10T_H$ at the same different times of Fig. 1, i.e., $t_1 = 1/\kappa$ (a), $t_2 = 2/\kappa$ (b), $t_3 = 4/\kappa$ (c), $t_4 = 5/\kappa$ (d).

$$M(v) = m\theta(v - v_0), \quad (3.2)$$

where m is a constant and θ is the Heaviside step function. So, inside the shell (i.e., $v < v_0$), we have Minkowski space-time

$$ds_{\text{in}}^2 = -dv^2 + 2dvdr + r^2 d\Omega^2, \quad (3.3)$$

where $d\Omega^2 = d\theta^2 + \sin^2\theta d\varphi^2$, while outside the shell (i.e., $v > v_0$), the metric is the Schwarzschild one describing a BH of mass m and horizon located at $r = 2m$:

$$ds^2 = -\left(1 - \frac{2m}{r}\right)dv^2 + 2dvdr + r^2 d\Omega^2. \quad (3.4)$$

Continuity of the induced metric on the shell ensures that the radial coordinate r is continuous across the shell. The resulting Penrose diagram of our space-time is given in Fig. 9.

In the interior region, we can introduce a retarded null coordinate u_{in} as

$$u_{\text{in}} = v - 2r \quad (3.5)$$

and write the Minkowski metric in a double-null form,

$$ds^2 = -du_{\text{in}}dv + r^2(u_{\text{in}}, v)d\Omega^2, \quad (3.6)$$

where

$$r(u_{\text{in}}, v) = \frac{v - u_{\text{in}}}{2}. \quad (3.7)$$

Similarly, in the external region, we define the retarded Eddington-Finkelstein null coordinate u as

$$u = v - 2r^*, \quad (3.8)$$

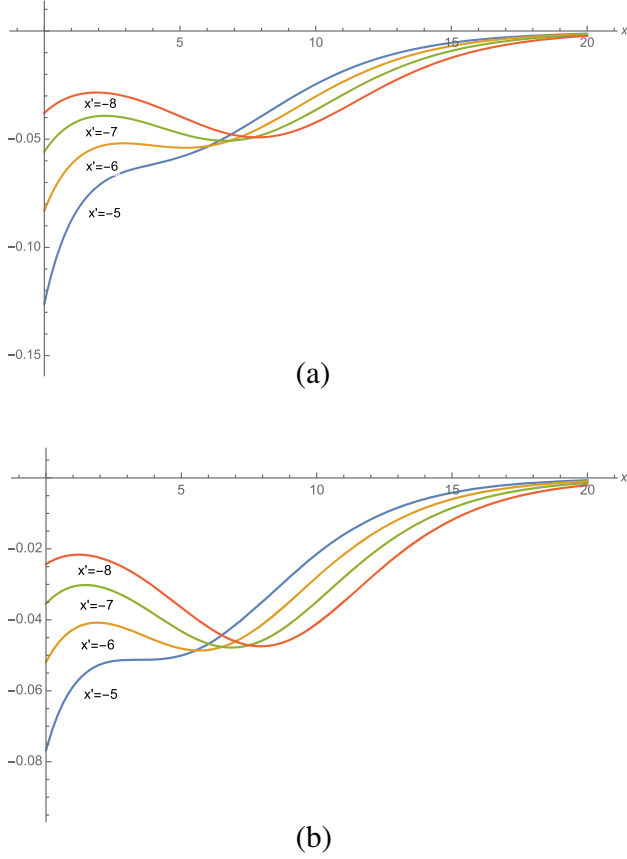


FIG. 8. Plots of $G_{2T}^{(1)}(t; x, x')$, $T = T_H$ in (a) and $T = 10T_H$ in (b), at $t = \frac{10}{\kappa}$ as a function of x for various values of x' as we did in Fig. 2 for the $T = 0$ case.

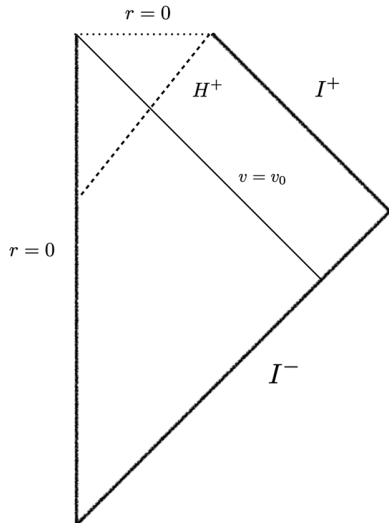


FIG. 9. Penrose diagram of a Schwarzschild black hole formed by a null shell collapse.

where r^* is the tortoise Regge-Wheeler coordinate

$$r^* = \int \frac{dr}{1 - \frac{2m}{r}} = r + 2m \ln \left| \frac{r}{2m} - 1 \right| \quad (3.9)$$

and the double-null form of the Schwarzschild metric reads

$$ds^2 = - \left(1 - \frac{2m}{r} \right) dudv + r^2(u, v) d\Omega^2, \quad (3.10)$$

where $r(u, v)$ is implicitly defined by

$$r^* = \frac{v - u}{2}. \quad (3.11)$$

Along the shell, we have $r(u_{\text{in}}, v_0) = r(u, v_0)$, and this leads to

$$u = u_{\text{in}} - 4m \ln \left| \frac{v_0 - 4m - u_{\text{in}}}{4m} \right|. \quad (3.12)$$

For simplicity, we set $v_0 = 4m$. This relation, once inverted as $u_{\text{in}}(u)$, allows us to extend the coordinate u_{in} in the exterior region. In particular, we have [30]

$$u_{\text{in}} = -4mW(\pm e^{-\frac{u}{4m}}), \quad (3.13)$$

where W is the Lambert function and $+$ holds in the region exterior to the horizon and $-$ in the interior one.

We consider now a quantized field $\hat{\phi}$, for simplicity scalar and massless, propagating in this space-time. The modes associated to this field are assumed to have the form $\frac{e^{-i\omega v}}{\sqrt{4\pi}\sqrt{2\pi\omega r}}$ on past null infinity I^- , and in this way, the quantum state of our field is Minkowski vacuum on I^- ; i.e., there are no incoming particles. We call this state $|in\rangle$. We neglect backscattering of the modes induced by the curvature of the space-time and simply impose reflecting conditions on the origin $r = 0$ in the Minkowski region yielding $u_{\text{in}} = v$ at $r = 0$ [see Eq. (3.7)] and requiring regularity of the modes there. This leads us to approximate our $(1+3)$ -dimensional theory as an effective $(1+1)$ -dimensional one describing a massless scalar field $\hat{\phi}$ propagating in the $(1+1)$ -dimensional space-time section of our space-time obtained by taking θ and φ constants, i.e.,

$$ds_{(2)}^2 = - \left(1 - \frac{2M(v)}{r} \right) dv^2 + 2dvdr. \quad (3.14)$$

This procedure is widely used in dealing with the Hawking effect for the Schwarzschild BH, allowing an analytical description which captures the essential physical features of the process. See, for instance, Refs. [18,31,32].

The two-point function corresponding to our $|in\rangle$ vacuum accounting for the boundary condition at $r = 0$ in the Minkowski region reads [33]

$$\langle \text{in} | \hat{\phi}(x) \hat{\phi}(x') | \text{in} \rangle = -\frac{\hbar}{4\pi} \ln \frac{(u_{\text{in}} - u'_{\text{in}})(v - v')}{(u_{\text{in}} - v')(u'_{\text{in}} - v)}. \quad (3.15)$$

In this section, we indicate with x the generic space-time point (t, r) . Unlike the previous case of an acoustic BH, space-time is now really curved, and this is affecting not just the quantum field $\hat{\phi}$ but also the observers which are requested to probe it. So, we have to specify not only the observable of the field $\hat{\phi}$ we want to measure but also which observer is going to measure it.

In the acoustic BH, one considers the density fluctuations measured by an observer at rest in the laboratory, which is an inertial observer in that case. To be as close as possible, we can choose the energy density of the field $\hat{\phi}$ as quantum observable, but one cannot choose observers at rest, since they do not exist inside the horizon and we are interested in correlations across the horizon which require measurements on both sides of it.

We therefore choose free-falling observers, moving on radial geodesics for simplicity. These are local inertial observers. So, our quantum observable is the scalar

$$\hat{\rho} \equiv \hat{T}_{ab} u^a u^b, \quad (3.16)$$

where

$$\hat{T}_{ab}(\hat{\phi}) = \partial_a \hat{\phi} \partial_b \hat{\phi} - \frac{g_{ab}}{2} g^{cd} \partial_c \hat{\phi} \partial_d \hat{\phi} \quad (3.17)$$

is the two-dimensional energy-momentum operator of the field $\hat{\phi}$ and u^a is the 4-velocity of the free-falling observer. Note that \hat{T}_{ab} is traceless due to the conformal invariance of $\hat{\phi}$ so it has only two independent components. The correlator we shall study is then

$$\langle \text{in} | \hat{\rho}(x) \hat{\rho}(x') | \text{in} \rangle \equiv G(x, x'), \quad (3.18)$$

evaluated in the Schwarzschild region where one point (x) is taken outside the horizon and the other (x') is taken inside.

Since in the acoustic BH the effective metric is given in Painlevé coordinates, we use the same coordinates here, transforming the original Schwarzschild metric (3.4) into

$$ds_{(2)}^2 = -f dt^2 - 2V dt dr + dr^2, \quad (3.19)$$

where $r = 1 - \frac{2m}{r} \equiv (1 - V^2)$, $V = -\sqrt{\frac{2m}{r}}$, and the Painlevé time t is given by

$$t = v + \int \left(\frac{\sqrt{1-f}}{f} - \frac{1}{f} \right) dr. \quad (3.20)$$

The metric (3.19) holds for points (t, r) such that $v(t, r) > v_0$, where $v(t, r)$ is obtained inverting (3.20). t is a regular time coordinate across the horizon. With this

choice, we can slice the entire BH space-time by constant t hypersurfaces similarly with what we did for the acoustic BH.¹

As shown in Appendix B, the energy density measured by a free-falling observer in Painlevé coordinates is simply

$$\hat{\rho}(t, r) = \hat{T}_{rr}(\hat{\phi}). \quad (3.21)$$

Using Eq. (B7), we can write the density-density correlator as

$$\begin{aligned} G(x, x') = \langle \text{in} | & \frac{\hat{T}_{uu}(x) \hat{T}_{u'u'}(x')}{(1+V(x))^2 (1+V(x'))^2} \\ & + \frac{\hat{T}_{uu}(x) \hat{T}_{v'v'}(x')}{(1+V(x))^2 (1-V(x'))^2} \\ & + \frac{\hat{T}_{vv}(x) \hat{T}_{u'u'}(x')}{(1-V(x))^2 (1+V(x'))^2} \\ & + \frac{\hat{T}_{vv}(x) \hat{T}_{v'v'}(x')}{(1-V(x))^2 (1-V(x'))^2} | \text{in} \rangle. \end{aligned} \quad (3.22)$$

In Fig. 10, we plot the correlator $G(t, r; t', r')$ at equal Painlevé time (i.e., $t = t'$) for $0 < r' < 2m$ and $2m < r < 4m$ outside the shell. The sequence of figures corresponds to four increasing Painlevé times $t = 10m, 20m, 30m, 40m$.

The result is quite surprising: no structure at all appears.² The same conclusion is reached by representing the correlator at $t = t' = 40m$ as a function of r for different values of $r' < 2m$: $r' = 0.8m, m, 1.2m, 1.4m$. See Fig. 11.

So, it seems that there is no signal in the equal-time correlator (3.22) of the correlations between the Hawking particles and their partners, and this is in striking contradiction with our naive expectation and with what we found for the acoustic BH. A comparison of Figs. 1 and 2 of our previous section with the actual ones is clearly illustrating this discrepancy. For the acoustic BH, we found no sign of the correlations close to the horizon because there the correlator is dominated by the light cone (coincidence limit in the case of equal-time) singularity. Correlations appeared, however, well outside the horizon with the characteristic peak we saw. So, our expectation was to find a similar peak structure even in our gravitational BH for points sufficiently away from the horizon, in the quantum atmosphere region.

¹Instead of t , we can use as time parameter Eddington-Finkelstein time $t_{\text{EF}} = v - r$, which is also a regular time coordinate across the horizon, and slice the space-time accordingly. No qualitative difference emerges in the results we will obtain.

²Although all Figs. 10 seem the same, differences nevertheless exist away from the divergent coincident limit $r = r' = 2m$, but they are too small to be seen in these plots and are irrelevant for our discussion.

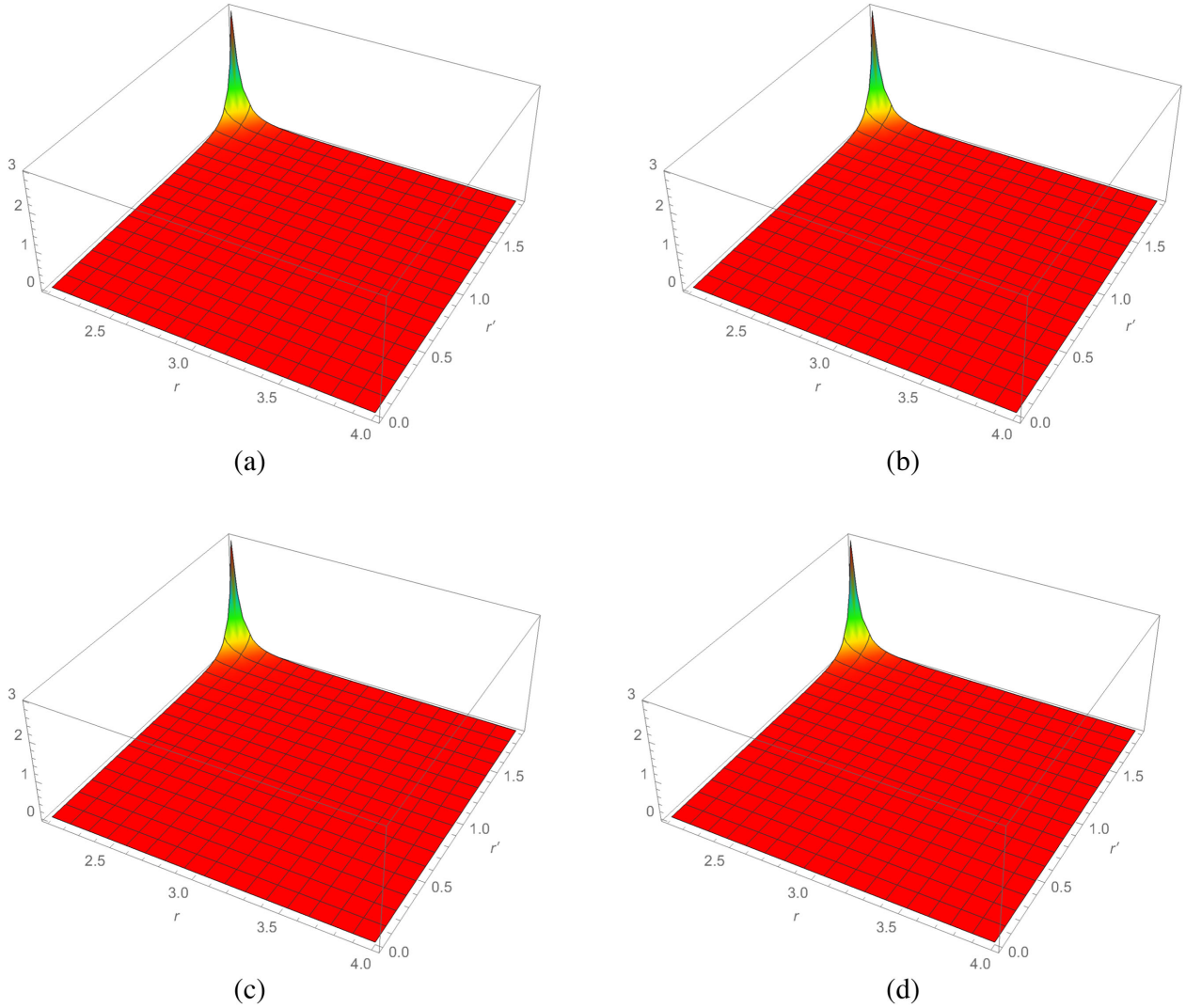


FIG. 10. Plot of $G(t, r; t', r')$ ($\hbar = 1, m = 1$ in all plots of this section) at equal Painlevé time for $0 < r' < 2m$ and $2m < r < 4m$ outside the shell at four increasing Painlevé times $t = 10m$ (a), $20m$ (b), $30m$ (c), $40m$ (d).

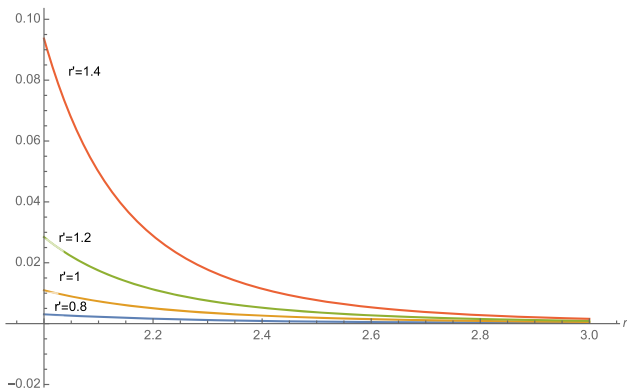


FIG. 11. $G(t, r; t', r')$ at $t = t' = 40m$ as a function of r at values of $r' < 2m$: $r' = 0.8m, m, 1.2m, 1.4m$.

So, one has to understand why this feature does not show up. At first sight, one could argue that this is an artifact related to the motion of the observers (free falling in our case) measuring the correlations affecting the result, while in the acoustic case, measurements are made at fixed laboratory coordinates. We do not think this is the case. If one calculates the equal-time density-density correlator of Eq. (2.6) for a hypothetical acoustic metric given by the Schwarzschild one of Eq. (3.4) for which $c = 1$ and the velocity profile is $V = -\sqrt{2m/r}$ (diverging at $r = 0$) and where the $r = 0$ singularity is replaced by a sink absorbing both the condensate atoms and the phonons, as discussed, for example, in Ref. [34], one would obtain the plot depicted in Fig. 12. The same negative result occurs: no peak in the equal-time correlation function.

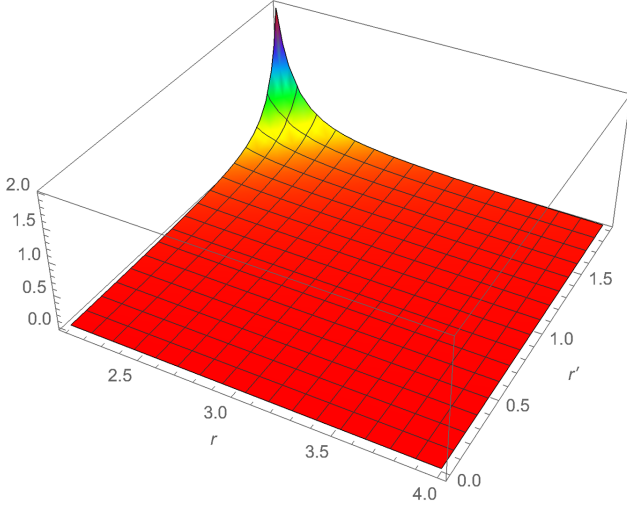


FIG. 12. Density correlator (2.6) for an hypothetical acoustic Schwarzschild metric.

Now, the key ingredient for the description of these correlations [see Eqs. (3.22), (B10), (B14)] is the correlator

$$\begin{aligned} & \frac{\partial_u \partial_{u'} \langle \text{in} | \hat{\phi}(x) \hat{\phi}(x') | \text{in} \rangle}{(1+V(r))(1+V(r'))} \Big|_{t=t'} \\ &= -\frac{\hbar}{4\pi(1+V(r))(1+V(r'))} \frac{u_{\text{in}} u'_{\text{in}}}{(u_{\text{in}} - u'_{\text{in}})^2} \\ & \quad \times \frac{1}{(u_{\text{in}} - 4m)(u'_{\text{in}} - 4m)} \Big|_{t=t'}, \end{aligned} \quad (3.23)$$

from which the relevant part of the density-density correlations [Eq. (3.22)] is constructed. Note its similarity with the $G_2^{(1)}(t; x, x')$ correlator of Eq. (2.6) in the acoustic case discussed in the previous section.

At late retarded time ($u \rightarrow +\infty, u_{\text{in}} \rightarrow 0$), we have, from (3.12), that the relation between u_{in} and u can be approximated as

$$u_{\text{in}} = \pm 4m e^{-\frac{u}{4m}}, \quad (3.24)$$

where $u_{\text{in}} < 0$ for $r > 2m$ and $u_{\text{in}} > 0$ for $r < 2m$. Using this, we get in this limit

$$\begin{aligned} & \frac{\partial_u \partial_{u'} \langle \text{in} | \hat{\phi}(x) \hat{\phi}(x') | \text{in} \rangle}{(1+V(r))(1+V(r'))} \Big|_{t=t'} \\ &= \frac{\hbar}{4\pi(1-\sqrt{\frac{2m}{r}})(1-\sqrt{\frac{2m}{r'}})} \frac{1}{16m^2 \cosh^2(\frac{u-u'}{8m})} \Big|_{t=t'}, \end{aligned} \quad (3.25)$$

which is extremized, for r, r' sufficiently away from the horizon, by $u = u'$ (i.e., along the trajectories of the particle and partner). Combining (3.8) and (3.20), we have

$$u = t - r - 2\sqrt{2mr} - 4m \ln \left| \sqrt{\frac{r}{2m}} - 1 \right|, \quad (3.26)$$

and so the condition $u = u'$ at equal times gives

$$\begin{aligned} & r + 2\sqrt{2mr} + 4m \ln \left(\sqrt{\frac{r}{2m}} - 1 \right) \\ &= r' + 2\sqrt{2mr'} + 4m \ln \left(1 - \sqrt{\frac{r'}{2m}} \right). \end{aligned} \quad (3.27)$$

So, in analogy with what we saw for the acoustic BH, one would expect that at late time for r, r' not sufficiently close to the horizon the equal-time density correlator $G(t; x, x')$ should show a peak along (3.27). If we plot the two functions entering the left- and right-hand sides of Eq. (3.27), as shown in Fig. 13, we see the critical point explaining the apparently absurd result of our Fig. 10: Eq. (3.27) has a solution only for $r \lesssim 2.6m$ for which the corresponding $r' > 0$. So, when the Hawking particle emerges from the quantum atmosphere out of the vacuum fluctuations, at a distance $O(1/\kappa)$ (where $\kappa = \frac{1}{4m}$ is the surface gravity of the Schwarzschild black hole) from the horizon, the corresponding partner has already been swallowed by the singularity, and the correlations are lost. On the other hand, for points (r, r') correlated by (3.27) with a nonvanishing $r' (< 2m)$, the density correlator $G(x, x')$ is dominated by the coincidence limit, and as happens for acoustic BHs, peaks do not appear. The behavior of $G(x, x')$ at equal times we found in Fig. 10 is completely understandable. To better appreciate the difference with the acoustic case, we have plotted in Fig. 14 the peak condition $u = u'$ for the acoustic metric (2.5), using Eq. (A9) at equal time. This has to be compared with Fig. 13 for the gravitational BH. The appearance at equal time of the peak in the acoustic case and the nonappearance in the gravitational case are self-evident.

To show the particle-partner correlation present in Hawking radiation, we have to consider the correlator $G(x, x')$ no longer at equal time but at t sufficiently bigger

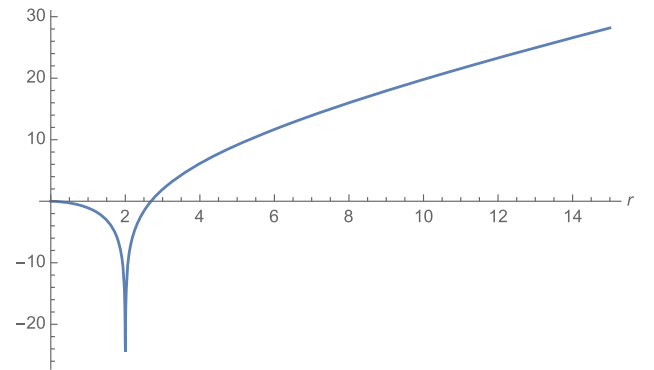


FIG. 13. Plot of the left- and right-hand sides of Eq. (3.27).

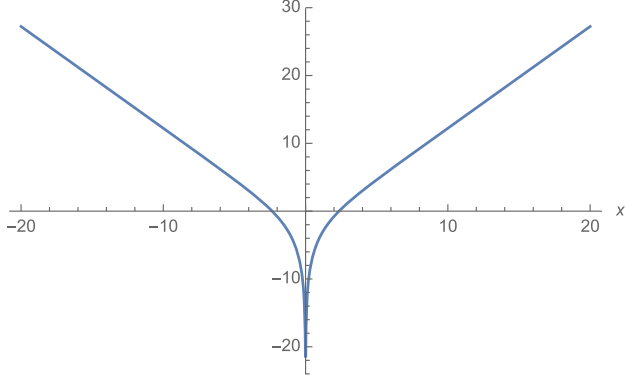


FIG. 14. Plot of the $u = u'$ condition at $t = t'$ in the acoustic case, with u given in (A9).

than t' so that the particle is sufficiently far away from the horizon while the partner has not yet been swallowed by the singularity. Indeed, we see in Fig. 15(a) the emergence of a characteristic peak structure, the locus of the peak, see Fig. 15(b), being compatible with the $u = u'$ condition.

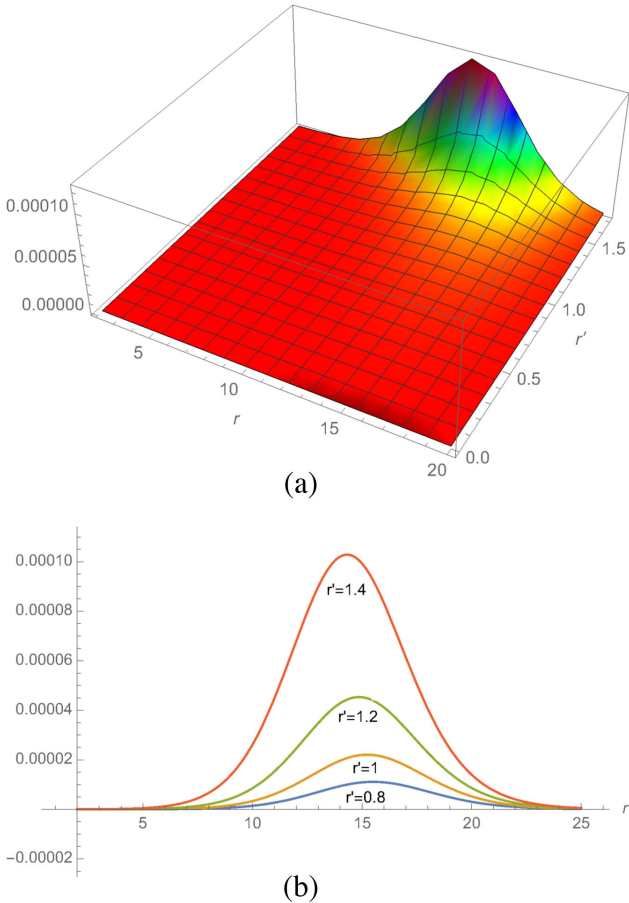


FIG. 15. (a) Three-dimensional plot of $G(x, x')$ at late time for $\Delta t = 30m$. (b) The same correlator for fixed $r' = 0.8m, m, 1.2m, 1.4m$.

For a condensed matter analog of this aspect, see Ref. [34], in which a proposal for an analog Schwarzschild BH by using condensates of light is made. That reference's Fig. 4 describes the expected signals in the correlation functions at unequal times.

For completeness, one has to say that if one considers just the $\langle \text{in} | T_{uu}(x) T_{u'u'}(x') | \text{in} \rangle$ correlator one finds a maximum confined close to the horizon. This very localized structure emerges because this correlator, unlike $G(x, x')$, vanishes when x or x' is on the horizon [see Eqs. (B11) and (B14)] for $u_{\text{in}} = 0$ or $u'_{\text{in}} = 0$, see also Ref. [26]. This is due to the pathological behavior of the u modes at the horizon. A similar argument holds for the $\frac{T_{uu}}{f}$ correlator.

IV. CONCLUSIONS

In this paper, we have used the methods of QFT in curved space to investigate a characteristic feature of Hawking BH radiation, namely, the quantum correlation across the horizon between the Hawking particles and their partners which should show the genuine pair creation mechanism at the origin of this effect. The analysis concerned both acoustic BHs formed by BECs, where the predicted correlations have indeed been experimentally observed [10,11], and the more standard BHs formed by gravitational collapse. We considered not just the late-time stationary regime, but following the time evolution of the correlations, we were able to find, in the acoustic BH case, where and when Hawking radiation appears once an horizon has formed [13]. The gravitational BH led us to a puzzling result: the characteristic peak in the equal-time correlation function, signaling the particle-partner correlations we found in the acoustic case, is absent here. The reason for this unexpected result lies in the presence of the BH central singularity. As we have seen, Hawking particles are produced in a region displaced from the horizon, the so-called quantum atmosphere. Once the Hawking particle emerges out of this region, the corresponding partner has already been swallowed by the singularity, and their mutual correlations are lost. Despite this negative result, we explicitly showed in Fig. 15 that the Hawking quanta-partner peak does indeed show up if we consider correlators at unequal times, allowing the Hawking particle to exit the quantum atmosphere region before its partner has reached the singularity.

Finally, as already mentioned in Sec. II, our results do not take into account the backscattering of the modes caused by the inhomogeneities in the metric. In the acoustic case, the effects of these inhomogeneities are to slightly alter (up to 10% [22]) the Hawking quanta-partner peak and to cause the appearance of two other signals in the correlation pattern related to the u - v scattering [23] and significantly smaller than the main signal. Needless to say, so far, only the signal corresponding to the Hawking quanta-partner peak has been observed in a BEC acoustic

BH. To discuss these two additional correlation channels for the Schwarzschild BH, a full four-dimensional analysis would be needed, which requires heavy numerical work to get the complete two-points function (see, for example, Refs. [35,36]) and which is outside the scope of the present paper.

ACKNOWLEDGMENTS

A. F. acknowledges partial financial support by the Spanish grants from Ministerio de Ciencia e Innovación No. FIS2017-84440-C2-1-P funded by Grant No. MCIN/AEI/10.13039/501100011033, “ERDF A way of making Europe,” Grant No. PID2020–116567 GB-C21 funded by Grant No. MCIN/AEI/10.13039/501100011033, and the Project No. PROMETEO/2020/079 (Generalitat Valenciana).

APPENDIX A: BEC BHS: DETAILS OF OUR MATHEMATICAL CONSTRUCTION

In this Appendix, we give the details for the mathematical construction of our BEC BH model of Sec. II.

In the 1 + 1-dimensional space-time described by the metric

$$ds^2 = -(c^2(t, x) - V^2)dt^2 - 2Vdtdx + dx^2 \quad (\text{A1})$$

with the speed of sound profile given by Eq. (2.1), we consider a massless scalar field $\delta\hat{\theta}^{(2)}(t, x)$ satisfying the field equation

$$\hat{\square}\delta\hat{\theta}^{(2)} = 0, \quad (\text{A2})$$

where $\hat{\square}$ is the d’Alembert operator calculated from the above metric. Since every (1 + 1) space-time is (locally) conformally flat, one can introduce a set of null coordinates (x^+, x^-) so that the metric can be written as

$$ds^2 = -C^2(x^+, x^-)dx^+dx^- \quad (\text{A3})$$

and the wave equation (A2) reduces simply to

$$\partial_{x^+}\partial_{x^-}\delta\hat{\theta}^{(2)} = 0. \quad (\text{A4})$$

The field operator $\delta\hat{\theta}^{(2)}$ can be expanded in modes as

$$\delta\hat{\theta}^{(2)} = \sum_{\omega} \left[\hat{a}_{\omega}^+ \frac{e^{-i\omega x^+}}{\sqrt{2\pi\omega}} + \hat{a}_{\omega}^- \frac{e^{-i\omega x^-}}{\sqrt{2\pi\omega}} + \text{H.c.} \right]. \quad (\text{A5})$$

The vacuum state $|0\rangle$ is defined as $\hat{a}_{\omega}^{\pm}|0\rangle = 0$, and the corresponding two-point function reads

$$\langle 0|\delta\hat{\theta}^{(2)}(x)\delta\hat{\theta}^{(2)}(x')|0\rangle = -\frac{\hbar}{4\pi} \ln \Delta x^+ \Delta x^-, \quad (\text{A6})$$

where $\Delta x^{\pm} = x^{\pm} - x'^{\pm}$. In Eq. (A6), we have omitted a diverging (irrelevant in our case) constant related to the IR

divergence of our (1 + 1) theory. The choice of null coordinates selects the conformal vacuum.

In our space-time, the set of null coordinates we choose for $t < 0$ is

$$u_{\text{in}} = t - \frac{x}{c_{\text{in}} - |V|}, \quad v_{\text{in}} = t + \frac{x}{c_{\text{in}} + |V|}. \quad (\text{A7})$$

The associated vacuum state, that we denote as $|in\rangle$, represents a quantum state in which for $t < 0$ there are no incoming quanta, both from left and right past null infinity. The corresponding two-point function is then

$$\begin{aligned} \langle 0|\delta\hat{\theta}^{(2)}(t, x)\delta\hat{\theta}^{(2)}(t', x')|0\rangle \\ = -\frac{\hbar}{4\pi} [\ln(u_{\text{in}} - u'_{\text{in}}) + \ln(v_{\text{in}} - v'_{\text{in}})], \end{aligned} \quad (\text{A8})$$

where $t, t' < 0$. The decoupling of the advanced (v_{in}) and retarded (u_{in}) sector is a consequence of the conformal invariance of the (1 + 1) massless theory.

We have now to analytically extend the above expression in the relevant BH region, i.e., for $t, t' > 0$. This is done by matching the null coordinates of Eq. (A7) with the corresponding ones in the BH region, namely,

$$u = t - \int \frac{dx}{c(x) - |V|} = t - \frac{1}{\kappa} \ln \sinh \frac{3\kappa|x|}{2|V|}, \quad (\text{A9})$$

$$\begin{aligned} v = t + \int \frac{dx}{c(x) + |V|} \\ = t + \frac{1}{8\kappa} \left[\frac{9\kappa x}{2|V|} - \ln \cosh \left(\frac{3\kappa x}{2|V|} + \tanh^{-1} \frac{1}{3} \right) \right], \end{aligned} \quad (\text{A10})$$

along the discontinuity at $t = 0$. See Fig. 16.

Starting with the retarded coordinates, from the first of (A7) at $t = 0$, we have

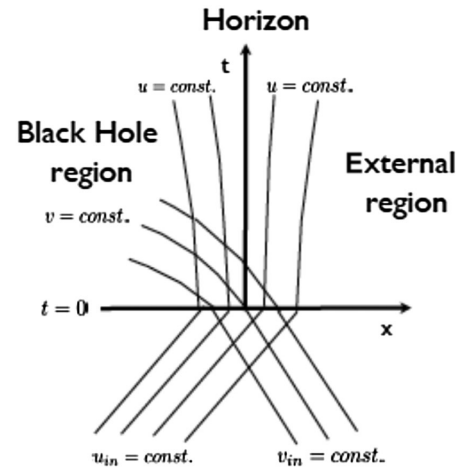


FIG. 16. Null coordinates matching (in the “in” and BH regions) at the $t = 0$ discontinuity.

$$u_{\text{in}} = -\frac{x}{c_{\text{in}} - |V|}. \quad (\text{A11}) \quad \text{We proceed similarly for the advanced null coordinates, obtaining}$$

Inserting this into (A9) evaluated at $t = 0$, we get

$$-\kappa u = \ln \sinh |Au_{\text{in}}|, \quad (\text{A12}) \quad v_{\text{in}} = \frac{4\kappa v}{B} + \frac{1}{2B} \ln \left(1 + \sqrt{1 + 2\sqrt{2}e^{-8\kappa v}} \right), \quad (\text{A15})$$

where

$$A = \frac{3\kappa}{2|V|} (|V| - c_{\text{in}}) < 0. \quad (\text{A13})$$

where

$$B = \frac{3\kappa(c_{\text{in}} + |V|)}{2|V|}. \quad (\text{A16})$$

The relation can be inverted giving

$$|u_{\text{in}}A| = \ln \left(\sqrt{1 + e^{-2\kappa u}} + e^{-\kappa u} \right). \quad (\text{A14}) \quad \text{So, the two-point function for } t, t' > 0 \text{ can be written formally as}$$

$$\langle 0 | \delta \hat{\theta}^{(2)}(t, x) \delta \hat{\theta}^{(2)}(t', x') | 0 \rangle = -\frac{\hbar}{4\pi} \{ \ln[u_{\text{in}}(u(t, x)) - u'_{\text{in}}(u'(t', x'))] + \ln[v_{\text{in}}(v(t, x)) - v'_{\text{in}}(v'(t', x'))] \}, \quad (\text{A17})$$

where $u_{\text{in}}(u(t, x))$ is given by Eqs. (A14) and (A9) and $v_{\text{in}}(v(t, x))$ is given by Eqs. (A15) and (A10).

We have, now, all that is needed to compute the density-density equal-time correlator [see Eq. (2.2)]

$$G_2^{(1)}(t; x, x') = \frac{n(x)n(x')}{m^2 c^2(x)c^2(x')} \lim_{t \rightarrow t'} \sqrt{\frac{m^2 c(x)c(x')}{n(x)n(x')}} D \langle \delta \hat{\theta}^{(2)}(t, x) \delta \hat{\theta}^{(2)}(t', x') \rangle, \quad (\text{A18})$$

where the differential operator D is defined in Eq. (2.3), giving

$$\begin{aligned} G_2^{(1)}(t; x, x') &= -\frac{\hbar n}{4\pi m c(x)^{1/2} c(x')^{1/2}} \left[\frac{1}{(c(x) - |V|)(c(x') - |V|)} \frac{du_{\text{in}}}{du} \frac{du'_{\text{in}}}{du'} \frac{1}{(u_{\text{in}} - u'_{\text{in}})^2} \right. \\ &\quad \left. + \frac{1}{(c(x) + |V|)(c(x') + |V|)} \frac{dv_{\text{in}}}{dv} \frac{dv'_{\text{in}}}{dv'} \frac{1}{(v_{\text{in}} - v'_{\text{in}})^2} \right] \Big|_{t=t'} \\ &\equiv G_{2,u}^{(1)}(t; x, x') + G_{2,v}^{(1)}(t; x, x'), \end{aligned} \quad (\text{A19})$$

where

$$\begin{aligned} G_{2,u}^{(1)}(t; x, x') &= -\frac{\hbar n}{4\pi m} \frac{\kappa^2}{|V|^3} \frac{1}{\sqrt{\left(1 + \frac{2}{3} \tanh \frac{3\kappa x}{2|V|}\right)^2 \tanh \frac{3\kappa x}{2|V|}}} \frac{1}{\sqrt{\left(1 + \frac{2}{3} \tanh \frac{3\kappa x'}{2|V|}\right)^2 \tanh \frac{3\kappa x'}{2|V|}}} \\ &\quad \times \frac{e^{-2\kappa t} \sinh \frac{3\kappa x}{2|V|} \sinh \frac{3\kappa x'}{2|V|}}{\sqrt{\left(1 + e^{-2\kappa t} \sinh^2 \frac{3\kappa x}{2|V|}\right) \left(1 + e^{-2\kappa t} \sinh^2 \frac{3\kappa x'}{2|V|}\right)}} \left(\frac{1}{\ln \frac{\sqrt{1 + e^{-2\kappa t} \sinh^2 \frac{3\kappa x}{2|V|}} + e^{-\kappa t} \sinh \frac{3\kappa x}{2|V|}}{\sqrt{1 + e^{-2\kappa t} \sinh^2 \frac{3\kappa x'}{2|V|}} + e^{-\kappa t} \sinh \frac{3\kappa x'}{2|V|}}} \right)^2 \end{aligned} \quad (\text{A20})$$

and

$$\begin{aligned}
G_{2,v}^{(1)}(t; x, x') = & -\frac{\hbar n}{4\pi m} \frac{1}{|V|^3} \frac{1}{\sqrt{(1 + \frac{2}{3} \tanh \frac{3\kappa x}{2|V|})(2 + \frac{2}{3} \tanh \frac{3\kappa x}{2|V|})}} \frac{1}{\sqrt{(1 + \frac{2}{3} \tanh \frac{3\kappa x'}{2|V|})(2 + \frac{2}{3} \tanh \frac{3\kappa x'}{2|V|})}} \\
& \times \frac{\sqrt{1 + e^{-8\kappa t - \frac{9\kappa x}{2|V|}}(2e^{\frac{3\kappa x}{2|V|}} + e^{-\frac{3\kappa x}{2|V|}})} + 1 + \frac{1}{2} e^{-8\kappa t - \frac{9\kappa x}{2|V|}}(2e^{\frac{3\kappa x}{2|V|}} + e^{-\frac{3\kappa x}{2|V|}})}{\sqrt{1 + e^{-8\kappa t - \frac{9\kappa x}{2|V|}}(2e^{\frac{3\kappa x}{2|V|}} + e^{-\frac{3\kappa x}{2|V|}})}(1 + \sqrt{1 + e^{-8\kappa t - \frac{9\kappa x}{2|V|}}(2e^{\frac{3\kappa x}{2|V|}} + e^{-\frac{3\kappa x}{2|V|}})})} \\
& \times \frac{\sqrt{1 + e^{-8\kappa t - \frac{9\kappa x'}{2|V|}}(2e^{\frac{3\kappa x'}{2|V|}} + e^{-\frac{3\kappa x'}{2|V|}})} + 1 + \frac{1}{2} e^{-8\kappa t - \frac{9\kappa x'}{2|V|}}(2e^{\frac{3\kappa x'}{2|V|}} + e^{-\frac{3\kappa x'}{2|V|}})}{\sqrt{1 + e^{-8\kappa t - \frac{9\kappa x'}{2|V|}}(2e^{\frac{3\kappa x'}{2|V|}} + e^{-\frac{3\kappa x'}{2|V|}})}(1 + \sqrt{1 + e^{-8\kappa t - \frac{9\kappa x'}{2|V|}}(2e^{\frac{3\kappa x'}{2|V|}} + e^{-\frac{3\kappa x'}{2|V|}})})} \\
& \times \frac{1}{\left(\frac{9}{16|V|} (x - x') - \frac{1}{8\kappa} \ln \frac{2e^{\frac{3\kappa x}{2|V|}} + e^{-\frac{3\kappa x}{2|V|}}}{2e^{\frac{3\kappa x'}{2|V|}} + e^{-\frac{3\kappa x'}{2|V|}}} + \frac{1}{8\kappa} \ln \frac{1 + \sqrt{1 + e^{-8\kappa t - \frac{9\kappa x}{2|V|}}(2e^{\frac{3\kappa x}{2|V|}} + e^{-\frac{3\kappa x}{2|V|}})}}{1 + \sqrt{1 + e^{-8\kappa t - \frac{9\kappa x'}{2|V|}}(2e^{\frac{3\kappa x'}{2|V|}} + e^{-\frac{3\kappa x'}{2|V|}})}} \right)^2} \quad (A21)
\end{aligned}$$

correspond to the u channel (where Hawking radiation appears) and the v channel, respectively.

We can characterize a late-time limit in which stationarity is achieved by

$$e^{-\kappa t} \sinh \frac{3\kappa|x|}{2|V|} \ll 1, \quad (A22)$$

i.e.,

$$t_{\text{late time}} \gg \frac{1}{\kappa} \ln \sinh \frac{3\kappa|x|}{2|V|}, \quad (A23)$$

and it is clear that this time depends on the point chosen. One reaches a stationary regime earlier near the horizon ($x \simeq 0$) and later away from it. The stationary limit of Eq. (A20) then reads

$$G_{2,u}^{(1)}(t; x, x') = \frac{\hbar}{4\pi m n_0} \frac{\kappa^2}{|V|^3} \frac{1}{\sqrt{(1 + \frac{2}{3} \tanh \frac{3\kappa x}{2|V|})(\frac{2}{3} \tanh \frac{3\kappa x}{2|V|})}} \frac{1}{\sqrt{(1 + \frac{2}{3} \tanh \frac{3\kappa x'}{2|V|})(\frac{2}{3} \tanh \frac{3\kappa x'}{2|V|})}} \frac{1}{4 \cosh^2 \left(\frac{1}{2} \ln \frac{\sinh \frac{3\kappa x}{2|V|}}{\sinh \frac{3\kappa x'}{2|V|}} \right)}, \quad (A24)$$

while that of (A21) is

$$\begin{aligned}
G_{2,v}^{(1)}(t; x, x') = & -\frac{\hbar n}{4\pi m |V|^3} \frac{1}{\sqrt{(1 + \frac{2}{3} \tanh \frac{3\kappa x}{2|V|})(2 + \frac{2}{3} \tanh \frac{3\kappa x}{2|V|})}} \frac{1}{\sqrt{(1 + \frac{2}{3} \tanh \frac{3\kappa x'}{2|V|})(2 + \frac{2}{3} \tanh \frac{3\kappa x'}{2|V|})}} \\
& \times \frac{1}{\left(\frac{9}{16|V|} (x - x') - \frac{1}{8\kappa} \ln \frac{2e^{\frac{3\kappa x}{2|V|}} + e^{-\frac{3\kappa x}{2|V|}}}{2e^{\frac{3\kappa x'}{2|V|}} + e^{-\frac{3\kappa x'}{2|V|}}} \right)^2}. \quad (A25)
\end{aligned}$$

Instead of the initial vacuum state described by $|in\rangle$ in which there are no incoming quanta, we can consider the case in which the condensate has an initial temperature T so that we have an initial thermal distribution of phonons characterized by an occupation number

$$N_{\omega_{u(v)}} = \frac{1}{e^{\frac{\hbar\omega_{u(v)}}{k_B T}} - 1}, \quad (A26)$$

where the Doppler rescaled frequencies are

$$\omega_u = \frac{\omega C_{in}}{c_{in} - |V|}, \quad \omega_v = \frac{\omega C_{in}}{c_{in} + |V|} \quad (A27)$$

and k_B is the Boltzmann constant. The corresponding two-point function for this thermal state, that we denote by $|T\rangle$, for the quantum field $\delta\hat{\theta}^{(2)}$ is [37]

$$\langle T|\delta\hat{\theta}^{(2)}(t, x)\delta\hat{\theta}^{(2)}(t', x')|T\rangle = -\frac{\hbar}{4\pi} \ln \frac{\sinh A_u \Delta u_{\text{in}} \sinh A_v \Delta v_{\text{in}}}{A_u A_v}, \quad (\text{A28})$$

where

$$A_{u(v)} = \frac{\pi k_B T (c_{\text{in}} \mp |V|)}{\hbar c_{\text{in}}}, \quad (\text{A29})$$

the minus sign in (A29) corresponds to A_u , and the plus sign corresponds to A_v ; $\Delta u_{\text{in}} = u_{\text{in}} - u'_{\text{in}}$, $\Delta v_{\text{in}} = v_{\text{in}} - v'_{\text{in}}$. The thermal equal-time density-density correlator now reads

$$G_{2,T}^{(1)}(t; x, x') = -\frac{\hbar n^{(1)}}{4\pi m c(x)^{1/2} c(x')^{1/2}} \left[\frac{1}{(c(x) - |V|)(c(x') - |V|)} \frac{du_{\text{in}} du'_{\text{in}}}{du du'} \frac{A_u^2}{\sinh^2 A_u (u_{\text{in}} - u'_{\text{in}})} \right. \\ \left. + \frac{1}{(c(x) + |V|)(c(x') + |V|)} \frac{dv_{\text{in}} dv'_{\text{in}}}{dv dv'} \frac{A_v^2}{\sinh^2 A_v (v_{\text{in}} - v'_{\text{in}})} \right] \Big|_{t=t'}. \quad (\text{A30})$$

Separating the u and v channels, we have explicitly

$$G_{2,Tu}^{(1)}(t; x, x') = -\frac{\hbar n}{4\pi m |V|^3} \frac{1}{\sqrt{(1 + \frac{2}{3} \tanh \frac{3\kappa x}{2|V|})^2 \tanh \frac{3\kappa x}{2|V|}}} \frac{1}{\sqrt{(1 + \frac{2}{3} \tanh \frac{3\kappa x'}{2|V|})^2 \tanh \frac{3\kappa x'}{2|V|}}} \\ \times \frac{e^{-2\kappa t} \sinh \frac{3\kappa x}{2|V|} \sinh \frac{3\kappa x'}{2|V|}}{\sqrt{(1 + e^{-2\kappa t} \sinh^2 \frac{3\kappa x}{2|V|})(1 + e^{-2\kappa t} \sinh^2 \frac{3\kappa x'}{2|V|})}} \frac{(\frac{k_B \pi}{\hbar \beta A} \frac{(c_{\text{in}} - |V|)}{c_{\text{in}}})^2}{\sinh^2 \left(\frac{k_B \pi}{\hbar \beta A} \frac{(c_{\text{in}} - |V|)}{c_{\text{in}}} \ln \frac{\sqrt{1 + e^{-2\kappa t} \sinh^2 \frac{3\kappa x}{2|V|} + e^{-\kappa t} \sinh \frac{3\kappa x}{2|V|}}}{\sqrt{1 + e^{-2\kappa t} \sinh^2 \frac{3\kappa x'}{2|V|} + e^{-\kappa t} \sinh \frac{3\kappa x'}{2|V|}}} \right)}} \quad (\text{A31})$$

and

$$G_{2,Tv}^{(1)}(t; x, x') = -\frac{\hbar n}{4\pi m |V|^3} \frac{1}{\sqrt{(1 + \frac{2}{3} \tanh \frac{3\kappa x}{2|V|})(2 + \frac{2}{3} \tanh \frac{3\kappa x}{2|V|})}} \frac{1}{\sqrt{(1 + \frac{2}{3} \tanh \frac{3\kappa x'}{2|V|})(2 + \frac{2}{3} \tanh \frac{3\kappa x'}{2|V|})}} \\ \times \frac{\sqrt{1 + e^{-8\kappa t - \frac{9\kappa x}{2|V|}}(2e^{\frac{3\kappa x}{2|V|}} + e^{-\frac{3\kappa x}{2|V|}}) + 1 + \frac{1}{2} e^{-8\kappa t - \frac{9\kappa x}{2|V|}}(2e^{\frac{3\kappa x}{2|V|}} + e^{-\frac{3\kappa x}{2|V|}})}}{\sqrt{1 + e^{-8\kappa t - \frac{9\kappa x}{2|V|}}(2e^{\frac{3\kappa x}{2|V|}} + e^{-\frac{3\kappa x}{2|V|}}) \left(1 + \sqrt{1 + e^{-8\kappa t - \frac{9\kappa x}{2|V|}}(2e^{\frac{3\kappa x}{2|V|}} + e^{-\frac{3\kappa x}{2|V|}})} \right)}} \\ \times \frac{\sqrt{1 + e^{-8\kappa t - \frac{9\kappa x'}{2|V|}}(2e^{\frac{3\kappa x'}{2|V|}} + e^{-\frac{3\kappa x'}{2|V|}}) + 1 + \frac{1}{2} e^{-8\kappa t - \frac{9\kappa x'}{2|V|}}(2e^{\frac{3\kappa x'}{2|V|}} + e^{-\frac{3\kappa x'}{2|V|}})}}{\sqrt{1 + e^{-8\kappa t - \frac{9\kappa x'}{2|V|}}(2e^{\frac{3\kappa x'}{2|V|}} + e^{-\frac{3\kappa x'}{2|V|}}) \left(1 + \sqrt{1 + e^{-8\kappa t - \frac{9\kappa x'}{2|V|}}(2e^{\frac{3\kappa x'}{2|V|}} + e^{-\frac{3\kappa x'}{2|V|}})} \right)}} \\ \times \frac{(\frac{4\kappa}{B} \frac{k_B \pi}{\hbar \beta} \frac{(c_{\text{in}} + |V|)}{c_{\text{in}}})^2}{\sinh^2 \left(\frac{4\kappa}{B} \frac{k_B \pi}{\hbar \beta} \frac{(c_{\text{in}} + |V|)}{c_{\text{in}}} \left(\frac{9}{16|V|} (x - x') - \frac{1}{8\kappa} \ln \frac{2e^{\frac{3\kappa x}{2|V|} + e^{-\frac{3\kappa x}{2|V|}}}}{2e^{\frac{3\kappa x'}{2|V|} + e^{-\frac{3\kappa x'}{2|V|}}}} + \frac{1}{8\kappa} \ln \frac{1 + \sqrt{1 + e^{-8\kappa t - \frac{9\kappa x}{2|V|}}(2e^{\frac{3\kappa x}{2|V|}} + e^{-\frac{3\kappa x}{2|V|}})}}}{1 + \sqrt{1 + e^{-8\kappa t - \frac{9\kappa x'}{2|V|}}(2e^{\frac{3\kappa x'}{2|V|}} + e^{-\frac{3\kappa x'}{2|V|}})}} \right)} \right)}} \quad (\text{A32})$$

Note that by introducing the Hawking temperature $T_H = \frac{\hbar \kappa}{2\pi k_B}$ we can rewrite the prefactor of the \ln in Eq. (A31), see also (A13), as $\frac{k_B \pi}{\hbar \beta A} \frac{(c_{\text{in}} - |V|)}{c_{\text{in}}} = -\frac{T}{T_H} \frac{|V|}{3c_{\text{in}}}$, and, in (32), see also (A16), $\frac{4\kappa}{B} \frac{k_B \pi}{\hbar \beta} \frac{(c_{\text{in}} + |V|)}{c_{\text{in}}} = \frac{T}{T_H} \frac{4|V|\kappa}{3c_{\text{in}}}$. We see that stationarity of $G_{2,Tu}^{(1)}$ is reached when $T > \frac{3c_{\text{in}}}{|V|} T_H$ not just by the previous condition $e^{-\kappa t} \sinh \frac{3\kappa|x|}{2|V|} \ll 1$, which holds for $T < \frac{3c_{\text{in}}}{|V|} T_H$, but by the most stringent condition

$$\frac{T}{\frac{3c_{\text{in}}}{|V|} T_H} e^{-\kappa t} \sinh \frac{3\kappa|x|}{2|V|} \ll 1. \quad (\text{A33})$$

The denominator of the last term in (A31) can be approximated as follows:

$$\begin{aligned} & \sinh^2 \left(\frac{k_B \pi}{\hbar \beta A} \frac{(c_{\text{in}} - |V|)}{c_{\text{in}}} \ln \frac{\sqrt{1 + e^{-2\kappa t} \sinh^2 \frac{3\kappa x}{2|V|}} + e^{-\kappa t} \sinh \frac{3\kappa x}{2|V|}}{\sqrt{1 + e^{-2\kappa t} \sinh^2 \frac{3\kappa x'}{2|V|}} + e^{-\kappa t} \sinh \frac{3\kappa x'}{2|V|}} \right) \\ & \simeq \sinh^2 \left(\frac{k_B \pi}{\hbar \beta A} \frac{(c_{\text{in}} - |V|)}{c_{\text{in}}} e^{-\kappa t} \left(\sinh \frac{3\kappa x}{2|V|} - \sinh \frac{3\kappa x'}{2|V|} \right) \right) \\ & \simeq \left(\frac{k_B \pi}{\hbar \beta A} \frac{(c_{\text{in}} - |V|)}{c_{\text{in}}} \right)^2 e^{-2\kappa t} \left(\sinh \frac{3\kappa x}{2|V|} - \sinh \frac{3\kappa x'}{2|V|} \right)^2. \end{aligned} \quad (\text{A34})$$

Inserting this in Eq. (A31) and approximating $\sqrt{1 + e^{-2\kappa t} \sinh^2 \frac{3\kappa x}{2|V|}} \simeq 1$, we have

$$G_{2,Tu}^{(1)}(t; x, x') = -\frac{\hbar n}{4\pi m} \frac{\kappa^2}{|V|^3} \frac{1}{\sqrt{(1 + \frac{2}{3} \tanh \frac{3\kappa x}{2|V|}) \frac{2}{3} \tanh \frac{3\kappa x}{2|V|}}} \frac{1}{\sqrt{(1 + \frac{2}{3} \tanh \frac{3\kappa x'}{2|V|}) \frac{2}{3} \tanh \frac{3\kappa x'}{2|V|}}} \frac{\sinh \frac{3\kappa x}{2|V|} \sinh \frac{3\kappa x'}{2|V|}}{(\sinh \frac{3\kappa x}{2|V|} - \sinh \frac{3\kappa x'}{2|V|})^2} \quad (\text{A35})$$

which (for points x, x' situated on both sides of the horizon) is exactly the same as the one at $T = 0$; see Eq. (A24). One can for completeness evaluate the late-time limit of $G_{2,Tv}^{(1)}$, giving

$$\begin{aligned} G_{2,Tv}^{(1)}(t; x, x') &= -\frac{\hbar n}{4\pi m} \frac{1}{|V|^3} \frac{1}{\sqrt{(1 + \frac{2}{3} \tanh \frac{3\kappa x}{2|V|})(2 + \frac{2}{3} \tanh \frac{3\kappa x}{2|V|})}} \frac{1}{\sqrt{(1 + \frac{2}{3} \tanh \frac{3\kappa x'}{2|V|})(2 + \frac{2}{3} \tanh \frac{3\kappa x'}{2|V|})}} \\ & \times \frac{\left(\frac{4\kappa \pi}{B \beta} \frac{(c_{\text{in}} + |V|)}{c_{\text{in}}} \right)^2}{\sinh^2 \left(\frac{4\kappa \pi}{B \beta} \frac{(c_{\text{in}} + |V|)}{c_{\text{in}}} \left(\frac{9}{16|V|} (x - x') - \frac{1}{8\kappa} \ln \frac{2e^{\frac{3\kappa x}{2|V|}} + e^{-\frac{3\kappa x}{2|V|}}}{2e^{\frac{3\kappa x'}{2|V|}} + e^{-\frac{3\kappa x'}{2|V|}}} \right) \right)}. \end{aligned} \quad (\text{A36})$$

APPENDIX B: GRAVITATIONAL BHS: DETAILS OF OUR MATHEMATICAL CONSTRUCTION

The Schwarzschild metric in Painlevé coordinates is (we consider the two-dimensional section)

$$ds^2 = -f dt^2 - 2V dt dr + dr^2. \quad (\text{B1})$$

The components of the 4-velocity of a geodesic observer freely falling from infinity with initial zero velocity are

$$u^a = (1, V). \quad (\text{B2})$$

So,

$$\hat{T}_{ab} u^a u^b = \hat{T}_{tt} + 2V \hat{T}_{rt} + V^2 \hat{T}_{rr}. \quad (\text{B3})$$

The vanishing of the trace of \hat{T}_{ab} gives

$$g^{ab} \hat{T}_{ab} = -\hat{T}_{tt} - 2V \hat{T}_{tr} + f \hat{T}_{rr} = 0, \quad (\text{B4})$$

which, inserted in Eq. (B3), gives

$$\hat{T}_{ab} u^a u^b = \hat{T}_{rr}. \quad (\text{B5})$$

Given the form of the two-point function [see Eq. (3.15)], it is useful for the calculations to express \hat{T}_{rr} in terms of \hat{T}_{uu} and \hat{T}_{vv} (note that $\hat{T}_{uv} = 0$), where u, v are Eddington-Finkelstein null coordinates. Performing the coordinate transformation, we have

$$\hat{T}_{rr}(t, r) = \left[\frac{\sqrt{1-f} + 1}{f} \right]^2 \hat{T}_{uu}(u, v) + \left[\frac{\sqrt{1-f} - 1}{f} \right]^2 \hat{T}_{vv}(u, v), \quad (\text{B6})$$

which, taking into account that $f = 1 - V^2$, $V < 0$, yields

$$\hat{T}_{rr} = \frac{\hat{T}_{uu}}{(1+V)^2} + \frac{\hat{T}_{vv}}{(1-V)^2}, \quad (\text{B7})$$

where $V = -\sqrt{\frac{2m}{r}}$.

From (3.17), we have

$$\hat{T}_{uu} = \partial_u \hat{\phi} \partial_u \hat{\phi}, \quad (\text{B8})$$

and similarly

$$\hat{T}_{vv} = \partial_v \hat{\phi} \partial_v \hat{\phi}. \quad (\text{B9})$$

The fundamental object for our calculation is

$$\partial_u \partial_{u'} \langle \text{in} | \hat{\phi}(x) \hat{\phi}(x') | \text{in} \rangle = -\frac{\hbar}{4\pi} \frac{du_{\text{in}}}{du} \frac{du'_{\text{in}}}{du'} \frac{1}{(u_{\text{in}} - u'_{\text{in}})^2}, \quad (\text{B10})$$

where use of the two-point function (3.15) was made. From this, the correlator of \hat{T}_{uu} reads formally

$$\langle \text{in} | \hat{T}_{uu}(x) \hat{T}_{u'u'}(x') | \text{in} \rangle = (\partial_u \partial_{u'} \langle \text{in} | \hat{\phi}(x) \hat{\phi}(x') | \text{in} \rangle)^2. \quad (\text{B11})$$

For the v sector,

$$\partial_v \partial_{v'} \langle \text{in} | \hat{\phi}(x) \hat{\phi}(x') | \text{in} \rangle = -\frac{\hbar}{4\pi} \frac{1}{(v - v')^2}, \quad (\text{B12})$$

so

$$\langle \text{in} | \hat{T}_{vv}(x) \hat{T}_{v'v'}(x') | \text{in} \rangle = \frac{\hbar}{(4\pi)^2} \frac{1}{(v - v')^4}. \quad (\text{B13})$$

Taking into account the relation between u and u' [see Eq. (3.12)], we can rewrite (B10) as

$$\begin{aligned} \partial_u \partial_{u'} \langle \text{in} | \hat{\phi}(x) \hat{\phi}(x') | \text{in} \rangle &= -\frac{\hbar}{4\pi} \frac{u_{\text{in}} u'_{\text{in}}}{(u_{\text{in}} - u'_{\text{in}})^2} \frac{1}{(u_{\text{in}} - 4m)(u'_{\text{in}} - 4m)} \\ &= -\frac{\hbar}{4\pi} \frac{1}{4 \cosh^2 \ln \sqrt{\frac{-u_{\text{in}}}{u'_{\text{in}}}}} \frac{1}{(u_{\text{in}} - 4m)(u'_{\text{in}} - 4m)}, \end{aligned} \quad (\text{B14})$$

where we have chosen the point x outside the horizon ($u_{\text{in}} < 0$) and x' inside the horizon ($u'_{\text{in}} > 0$) [more precisely, see Eq. (3.13)],

$$u_{\text{in}} = -4mW(e^{-\frac{u}{4m}}), \quad u'_{\text{in}} = -4mW(e^{-\frac{u'}{4m}}). \quad (\text{B15})$$

We see that the v sector gives just vacuum correlations. The correlations in Hawking radiation come only from the u sector, and this is a consequence of the conformal invariance of our model, which does not take into account backscattering of the modes of the quantum field. The mixed correlator can be similarly computed,

$$\langle \text{in} | \hat{T}_{uu}(x) \hat{T}_{v'v'}(x') | \text{in} \rangle = 2(\partial_u \partial_{v'} \langle \text{in} | \hat{\phi}(x) \hat{\phi}(x') | \text{in} \rangle)^2, \quad (\text{B16})$$

$$\langle \text{in} | \hat{T}_{vv}(x) \hat{T}_{u'u'}(x') | \text{in} \rangle = 2(\partial_v \partial_{u'} \langle \text{in} | \hat{\phi}(x) \hat{\phi}(x') | \text{in} \rangle)^2, \quad (\text{B17})$$

with

$$\partial_u \partial_{v'} \langle \text{in} | \hat{\phi}(x) \hat{\phi}(x') | \text{in} \rangle = -\frac{\hbar}{4\pi} \frac{u_{\text{in}}}{(u_{\text{in}} - 4m)} \frac{1}{(u_{\text{in}} - v')^2} \quad (\text{B18})$$

and

$$\partial_v \partial_{u'} \langle \text{in} | \hat{\phi}(x) \hat{\phi}(x') | \text{in} \rangle = -\frac{\hbar}{4\pi} \frac{u'_{\text{in}}}{(u'_{\text{in}} - 4m)} \frac{1}{(u'_{\text{in}} - v)^2}. \quad (\text{B19})$$

-
- [1] S. W. Hawking, *Nature (London)* **248**, 30 (1974); *Commun. Math. Phys.* **43**, 199 (1975).
[2] B. Carr, *Astrophys. J.* **201**, 1 (1975).
[3] T. N. Ukwatta, D. R. Stump, J. T. Linnemann, J. H. MacGibbon, S. S. Marinelli, T. Yapici, and K. Tollefson, *Astropart. Phys.* **80**, 90 (2016).
[4] S. Massar and R. Parentani, *Phys. Rev. D* **54**, 7426 (1996).
[5] W. Unruh, *Phys. Rev. Lett.* **46**, 1351 (1981).
[6] C. Barcelo, S. Liberati, and M. Visser, *Living Rev. Relativity* **8**, 12 (2005).
[7] L. J. Garay, J. R. Anglin, J. I. Cirac, and P. Zoller, *Phys. Rev. Lett.* **85**, 4643 (2000); *Phys. Rev. A* **63**, 023611 (2001).
[8] R. Balbinot, A. Fabbri, S. Fagnocchi, A. Recati, and I. Carusotto, *Phys. Rev. A* **78**, 021603 (2008).
[9] I. Carusotto, S. Fagnocchi, A. Recati, R. Balbinot, and A. Fabbri, *New J. Phys.* **10**, 103001 (2008).
[10] J. Steinhauer, *Nat. Phys.* **12**, 959 (2016).
[11] J. R. M. de Nova, K. Golubkov, V. I. Kolobov, and J. Steinhauer, *Nature (London)* **569**, 688 (2019).
[12] V. I. Kolobov, K. Golubkov, J. R. M. de Nova, and J. Steinhauer, *Nat. Phys.* **17**, 362 (2021).
[13] A. Fabbri and R. Balbinot, *Phys. Rev. Lett.* **126**, 111301 (2021).
[14] W. G. Unruh, *Phys. Rev. D* **15**, 365 (1977).
[15] S. B. Giddings, *Phys. Lett. B* **754**, 39 (2016).
[16] R. Dey, S. Liberati, and D. Pranzetti, *Phys. Lett. B* **774**, 308 (2017).
[17] R. Dey, S. Liberati, Z. Mirzaiyan, and D. Pranzetti, *Phys. Lett. B* **797**, 134828 (2019).
[18] P. C. W. Davies, S. A. Fulling, and W. G. Unruh, *Phys. Rev. D* **13**, 2720 (1976).
[19] R. Parentani, *Phys. Rev. D* **82**, 025008 (2010).
[20] F. Michel, J. F. Coupechoux, and R. Parentani, *Phys. Rev. D* **94**, 084027 (2016).
[21] L. P. Pitaevskii and S. Stringari, *Bose-Einstein Condensation* (Clarendon, Oxford, 2003).
[22] P. R. Anderson, R. Balbinot, A. Fabbri, and R. Parentani, *Phys. Rev. D* **87**, 124018 (2013).
[23] J. Macher and R. Parentani, *Phys. Rev. A* **80**, 043601 (2009).
[24] A. Recati, N. Pavloff, and I. Carusotto, *Phys. Rev. A* **80**, 043603 (2009).
[25] P.-E. Larré, A. Recati, I. Carusotto, and N. Pavloff, *Phys. Rev. A* **85**, 013621 (2012).
[26] R. Schutzhold and W. G. Unruh, *Phys. Rev. D* **81**, 124033 (2010).
[27] P. T. Chrusciel, J. L. Costa, and M. Heusler, *Living Rev. Relativity* **15**, 7 (2012).
[28] R. M. Wald, *Phys. Rev. D* **13**, 3176 (1976).
[29] A. Fabbri and J. Navarro-Salas, *Modeling Black Hole Evaporation* (Imperial College Press/World Scientific, London, 2005).
[30] M. R. R. Good, P. R. Anderson, and C. R. Evans, *Phys. Rev. D* **94**, 065010 (2016).
[31] R. Balbinot and A. Barletta, *Classical Quantum Gravity* **6**, 195 (1989).
[32] R. Parentani and T. Piran, *Phys. Rev. Lett.* **73**, 2805 (1994).
[33] B. A. Juárez-Aubry and J. Louko, *J. High Energy Phys.* **05** (2018) 140.
[34] L. Liao, E. C. I. van der Wurff, and D. van Oosten, *Phys. Rev. A* **99**, 023850 (2019).
[35] C. Buss and M. Casals, *Phys. Lett. B* **776**, 168 (2018).
[36] A. Lanir, A. Levi, A. Ori, and O. Sela, *Phys. Rev. D* **97**, 024033 (2018).
[37] F. Vendrell, *Helv. Phys. Acta* **70**, 598 (1997).